

# Near-term quantum algorithms for linear systems of equations

Hsin-Yuan Huang,<sup>1, 2,\*</sup> Kishor Bharti,<sup>3, †</sup> and Patrick Rebentrost<sup>3, ‡</sup>

<sup>1</sup>*Institute for Quantum Information and Matter, California Institute of Technology, USA*

<sup>2</sup>*Department of Computing and Mathematical Sciences, California Institute of Technology, USA*

<sup>3</sup>*Centre for Quantum Technologies, National University of Singapore, Singapore*

(Dated: December 21, 2024)

Solving linear systems of equations is an essential component in science and technology, including in many machine learning algorithms. Existing quantum algorithms have demonstrated large speedups in solving linear systems, but the required quantum resources are not available on near-term quantum devices. In this work, we study potential near-term quantum algorithms for linear systems of equations. We investigate the use of variational algorithms for solving  $Ax = b$  and analyze their optimization landscapes. We found that a wide range of variational algorithms designed to avoid barren plateaus, such as properly-initialized imaginary time evolution and adiabatic-inspired optimization, still suffer from a fundamentally different plateau problem. To circumvent this issue, we design a potentially near-term adaptive alternating algorithm based on a core idea: the classical combination of variational quantum states. We have conducted numerical experiments solving linear systems as large as  $2^{300} \times 2^{300}$  by considering special systems that can be simulated efficiently on a classical computer. These experiments demonstrate the algorithm's ability to scale to system sizes within reach in near-term quantum devices of about 100-300 qubits.

## I. INTRODUCTION

Quantum computing promises speedups for a set of problems including integer factoring and search. Speedups have also been discussed for finding approximate solutions to linear systems of equations and convex optimizations. Many of these algorithms require a large amount of low-decoherence and fully connected quantum bits, beyond the reach of near-term available quantum computing hardware. As near-term quantum devices approach sizes of 50 qubits and more, a large amount of research has been devoted to finding tasks where such devices can outperform classical computers. One area of research concerns so-called “quantum supremacy” [1–4], which is about exhibiting a task for which the classical simulation is conjectured to be hard but which is performed efficiently on a quantum device. While the theoretical guarantees are sound, usually such tasks do not have straightforward practical applications, such as in the case of Boson sampling [5] and IQP circuits [6]. On the other hand, many investigations focus on finding applications for near-term quantum computers. Such applications are believed to be in quantum chemistry, optimization and machine learning, and possible algorithmic candidates are the variational quantum eigensolver (VQE) [7–9] and quantum approximate optimization (QAOA) [10, 11]. A good definition of near-term quantum computing for applications is to find quantum algorithms that minimize the number of qubits, the number of layers of gates and the complexity of the quantum gates (in terms of controlled operations, for example,) and are tailored to the available hardware, while at the same time the problem should be of significant practical relevance.

Linear systems are important in a large variety of applications in engineering and the sciences. Generically, a linear system is specified by a non-square matrix  $A \in \mathbb{R}^{M \times N}$  and a right-hand side vector  $b \in \mathbb{R}^M$ . The task is to find a solution vector  $x \in \mathbb{R}^N$  for which  $Ax = b$ . Depending on the dimensions  $M$  and  $N$  and the rank of the matrix the task of solving the linear system takes on various forms. First, if the matrix is square and invertible, we can use matrix inversion to solve the linear system to find a unique solution. If the matrix is square and non-invertible, the pseudoinverse inverts only non-zero eigenvalues. If the matrix is non-square, we have the case of overdetermined and underdetermined equation systems. An overdetermined equation system appears for example in regression, where a few parameters, given by the vector  $x$ , are used to explain a larger amount of data points, specified by the vector  $b$ . In this case, no exact solution is possible and one often minimizes the  $\ell_2$  norm  $\|Ax - b\|_2^2$  to find the best solution. On the other hand if the equation system is underdetermined, an infinite set of solutions exists. Further constraints can be imposed to find specific solutions, such as minimizing the  $\ell_2$ -norm of the solution via the pseudoinverse, or achieving sparsity of the solution via additional  $\ell_0$  or  $\ell_1$  norm constraints, such as in LASSO estimator [12] or compressed sensing [13].

In this work, we study near-term quantum algorithms for solving linear systems. We start by analyzing the use of basic variational algorithms for this task. In variational algorithms, the quantum computer is used to prepare candidates for the solution vector, using a shallow sequence of parameterized unitaries. Then,

---

\*Electronic address: hsinyuan@caltech.edu

†Electronic address: kishor.bharti1@gmail.com

‡Electronic address: cqtfrp@nus.edu.sg

measurements are performed on the solution candidate to evaluate the quality of the candidate defined in terms of a loss function. Finally, an optimization loop updates the variational parameters to improve the quality of the solution candidate. We proposed two Ansätze for these basic variational algorithms. The first ones uses Ansätze that are hardware-efficient, and without explicit usage of the matrix  $A$  and  $b$ , hence is called the “Agnostic” Ansatz. Such Agnostic Ansätze can be used in various forms of optimization methods, such as Nelder-Mead method [14], imaginary-time evolution [15, 16], or adiabatic-inspired optimization [17]. The second Ansatz, an Alternating Operator Ansatz, is strongly dependent on the linear system and fully uses  $A$  and  $b$  via Hamiltonian simulation [18–22]. This approach is inspired by the adiabatic approach and the QAOA method. The drawback is the more far-term nature of the approach.

We then study the optimization landscape of the variational algorithms and discover potential problems in these variational algorithms. We found an interesting phenomenon showing that any pre-specified Ansatz with a polynomial number of variational parameters will have a plateau effect. This plateau effect originates from a different cause compared to the barren plateau issues discussed in [23], which comes from initializing the Ansatz with a deep enough random quantum circuit. We then analyze various efforts that circumvent the known barren plateau issue, such as properly-initialized imaginary time evolution or the adiabatic-inspired optimization. We show that these attempts still fall into the fundamentally different plateau effect. This analysis elucidates a potential caveat in variational algorithms to scale to larger system sizes and achieve quantum advantage. This plateau effect does not apply to the Alternating Operator Ansatz, but the more far-term property and the difficulty optimizing the parameters make it less appealing.

To provide a potential solution to the aforementioned problems, we pursue a different route and propose an adaptive alternating algorithm for solving linear systems on near-term quantum devices. This algorithm is based on a concept called Classical Combination of Variational Quantum States (abbreviated as CQS). As the name suggests, we show that different variational quantum states can be combined via classical pre- and post-processing to increase the power of near-term quantum computers. We show how to adaptively find a good set of variational quantum states and the optimal combination coefficients. This algorithm avoids difficulty in optimizing the variational parameters and provides some provable guarantee in solving linear systems, with some of the steps in the algorithm still relying on heuristics. A variation of this adaptive alternating algorithm can be created to achieve similar provable guarantee as existing quantum algorithms. It improves upon a recent work [24] by reducing the quantum gate count by  $(1/\epsilon)$ -fold, where  $\epsilon$  is the desired error to the optimal solution (e.g.,  $\epsilon = 0.01$ ), while using only one additional ancilla. To demonstrate the potential of this algorithm, we have conducted numerical simulations for solving linear systems with sizes up to  $2^{300} \times 2^{300}$ .

## II. CLASSICAL AND QUANTUM SETTING

We are given a Hermitian matrix  $A \in \mathbb{C}^{N \times N}$  with spectral radius  $\rho(A) \leq 1$ . Assume without loss of generality that  $N = 2^n$  and that  $A$  is invertible, i.e., all eigenvalues are non-zero. For non-Hermitian matrices, use the standard Hermitian embedding. Given a vector  $b \in \mathbb{C}^N$ , the main task is to find a vector  $x$  that solves the system of equations

$$Ax = b. \quad (1)$$

In the quantum setting, we have to make assumptions about the access to the linear system. First, we require quantum access to the right-hand side vector. The most natural assumption is that there exists a quantum circuit that prepares a quantum state proportional to the vector  $b$ .

**Assumption 1.** *Assume availability of an efficient quantum circuit described by the unitary  $U_b$  such that  $U_b|0\rangle^{\otimes n} = |b\rangle$ .*

Next, we require access to the matrix defining the linear system. Here, our main assumption is that the matrix is given by a small linear combination of known unitaries. This assumption is weaker than the assumption of an efficient Pauli decomposition.

**Assumption 2.** *Assume an efficient unitary decomposition of the matrix  $A \in \mathbb{C}^{N \times N}$ , i.e.  $A = \sum_{k=1}^{K_A} \beta_k U_k$ , with  $K_A = \mathcal{O}(\text{poly}(\log N))$  and unitaries  $U_k \in \mathbb{C}^{N \times N}$  with known quantum circuits. We can always absorb the phase of  $\beta_k$  into  $U_k$ , so we can assume  $\beta_k > 0$ .*

Next, we discuss the two main loss functions used in this work. The first loss function is the well-known  $\ell_2$ -norm loss used in regression methods.

**Definition 1.** *Let the linear system be given by  $A \in \mathbb{C}^{N \times M}$  and  $b \in \mathbb{C}^N$ . Define the loss function  $L_R(x) := \|Ax - b\|_2^2 = x^\dagger A^\dagger Ax - 2\text{Re}\{b^\dagger Ax\} + \|b\|_2^2$ .*

The second loss function is obtained by defining a Hamiltonian which has a unique ground state that is the solution to the linear system. This definition borrows techniques presented in [24] for solving the linear system via a method inspired by adiabatic quantum computation. To keep the adiabatic Hamiltonian positive across the adiabatic sweep, an ancilla has been introduced in Definition 2.

**Definition 2.** Let  $A \in \mathbb{R}^{N \times N}$  be symmetric and invertible with  $\rho(A) \leq 1$ . Define an extended matrix  $A(s) := (1 - s)Z \otimes \mathbb{1} + sX \otimes A$  and  $|+, b\rangle$ . In addition, define the parameterized Hamiltonian  $H(s) := A(s)P_{+,b}^\perp A(s)$ , with the projector  $P_{+,b}^\perp := \mathbb{1} - |+, b\rangle\langle+, b|$ .

Among other properties, in [24] it was shown that  $H(1)$  has a unique ground state with zero eigenvalue given by  $|+\rangle|x^*\rangle = |+\rangle\frac{A^{-1}|b\rangle}{\|A^{-1}|b\rangle\|_2}$ , which is proportional to the solution  $A^{-1}b$  after removing the ancilla. This Hamiltonian implies the following loss function.

**Definition 3.** Define the loss function  $L_H(|x\rangle) := \langle+, x|H(1)|+, x\rangle$ .

### III. VARIATIONAL ALGORITHMS AND ANSÄTZE

We first discuss basic variational algorithms for solving linear systems. A typical variational algorithm works as follows: one prepares multiple copies of a parameterized quantum state Ansatz and measures observables on it; the measurement results provide an estimate of the loss function. An optimization loop changes the parameters of the Ansatz with the goal of minimizing the loss function. In this section, we consider two types of variational Ansätze. Different Ansätze require different assumptions on the available hardware and can lead to different sets of solutions.

- **Agnostic Ansatz:** We take Ansätze which perform single qubit rotations and entangling operations. We do not take into account information of the linear system itself except by measuring the loss function.
- **Alternating Operator Ansatz:** We alternate the use of operators constructed from  $A$  and the vector  $|b\rangle$  for generating the Ansatz. This requires Hamiltonian simulation of operators derived from  $A$  and  $|b\rangle\langle b|$ .

In particular, we focus on minimizing the Hamiltonian loss function  $L_H(|x\rangle)$ , which is equivalent to finding the ground state of the Hamiltonian  $H(1)$ . This allows the use of tools such as variational quantum eigensolver in quantum chemistry to solve linear systems of equations. The detailed procedure to measure the Hamiltonian loss function is discussed in Appendix A.

#### A. Details on variational algorithms for optimizing the Ansatz

We first discuss the details of variational algorithms. We consider an Ansatz generated by a quantum circuit parametrized by  $\theta$ , i.e.,  $|\theta\rangle = U_{\text{Ansatz}}(\theta)|0\rangle^{\otimes n}$ . First, we show the basic variational quantum eigensolver (VQE) for finding the ground state of a Hamiltonian. Initialize the variational parameters  $\theta$  to be  $\theta_{\text{init}}$ . While  $\theta$  has not converged, do the following steps:

1. Prepare quantum state  $|\theta\rangle$  on the quantum computer.
2. Obtain an estimate for the loss function defined by  $\langle\theta|H|\theta\rangle$ .
3. Update  $\theta$  according to the obtained estimate of the loss function (e.g., using Nelder-Mead).

In addition to using Nelder-Mead, another strategy for optimizing the variational parameters is through the use of imaginary time propagation. Ideally, imaginary time propagation will move a given initial state to the ground state of the Hamiltonian as all excited states will be quickly suppressed. As Ref. [25] shows, instead of propagating the quantum system, one can directly propagate the parameters  $\theta$ . The detailed algorithm works as follows. Set  $\theta(0) = \theta_{\text{init}}$ . For  $t = 0, \delta t, 2\delta t, \dots, T$ , do the steps:

1. Obtain an estimate for all terms  $C_i(t)$  and  $M_{ij}(t)$  using copies of  $|\theta(t)\rangle$ , where  $M_{ij}(t) = \text{Re} \left\{ \left( \frac{\partial}{\partial \theta_i} |\theta(t)\rangle \right)^\dagger \frac{\partial}{\partial \theta_j} |\theta(t)\rangle \right\}$  and  $C_i(t) = \text{Re} \left\{ \left( \frac{\partial}{\partial \theta_i} |\theta(t)\rangle \right)^\dagger H(s) |\theta(t)\rangle \right\}$ .
2. Perform variational imaginary time propagation:  $\theta(t + \delta t) \leftarrow \theta(t) - M^{-1}(t)C(t)\delta t$ .

A more sophisticated approach is based on adiabatic evolution, where we gradually change the Hamiltonian  $H(s)$  from the initial Hamiltonian (at  $s = 0$ ) to the target Hamiltonian (at  $s = 1$ ). Such an adiabatic-assisted optimization was used in [26, 27]. We follow [27] and refer to this approach as the adiabatic-assisted VQE (AAVQE). To implement AAVQE, we discretize  $s$  into  $T$  adiabatic steps,  $s_0 = 0, s_1, \dots, s_{T-1}, s_T = 1$ . At each adiabatic step  $t$ , we use the optimized variational parameter  $\theta_{t-1}^*$  for  $H(s_{t-1})$  as the initial guess for  $H(s_t)$ . We first initialize  $\theta$  to be  $\theta_0^*$ , where  $|\theta_0^*\rangle$  is the ground state for the initial Hamiltonian  $H(0)$ . Then, for  $t = 1, \dots, T$ , we perform Nelder-Mead or imaginary time propagation on the parameter  $\theta$  to find an optimized variational parameter  $\theta_t^*$  for  $H(s_t)$  by starting from  $\theta_{t-1}^*$ .

## B. Agnostic Ansatz

We consider a pre-specified Ansatz with several layers, where each layer consists of single-qubit rotation for every qubit and a set of controlled NOT (CNOT) gates for entangling different qubits. The variational parameters are the rotation angles in the single-qubit rotations. This Ansatz does not take explicit account of the linear systems  $A, b$  and hence we use the name Agnostic Ansatz. We have performed numerical experiments on the Rigetti quantum virtual machine [28] with system sizes up to  $N = 16$  and explored various patterns of how the CNOT gates are applied. We observed that most CNOT gate patterns could find the solution as one increases the number of layers, and hence also increases the number of variational parameters. We have also tested the adiabatic-assisted VQE algorithm [26, 27]. The average accuracy (average fidelity of the output vector with the actual solution over randomly generated linear systems) approaches unity as one increases the number of adiabatic steps. We also observed improvement of adiabatic-assisted VQE over standard VQE. For plots and detailed findings, please refer to Appendix D.

## C. Alternating Operator Ansatz

We now discuss a different Ansatz that contains information about the linear system, i.e., the matrix  $A$  and the vector  $b$ . This Ansatz comes at the cost of requiring Hamiltonian simulation of operators involving  $A$  and  $b$ . The Ansatz is inspired by the method presented in [24] for solving the linear system via adiabatic techniques. We can write out the Hamiltonian in Definition 2 as

$$H(s) = (1-s)^2 \mathbb{1} + s^2 \mathbb{1} \otimes A^2 - (1-s)^2 |-, b\rangle \langle -, b| - s^2 (\mathbb{1} \otimes A) |+, b\rangle \langle +, b| (\mathbb{1} \otimes A) \\ - s(1-s) (|+, b\rangle \langle -, b| (\mathbb{1} \otimes A) + (\mathbb{1} \otimes A) |-, b\rangle \langle +, b|).$$

Examining the Hamiltonian leads to four Hermitian operators that make up  $H(s)$ , which are scaled by combinations of  $s$  and  $\pm(1-s)$ . The Hamiltonians are  $H_1 = A^2$ ,  $H_2 = |-, b\rangle \langle -, b|$ ,  $H_3 = (\mathbb{1} \otimes A) |+, b\rangle \langle +, b| (\mathbb{1} \otimes A)$ , and  $H_4 = |+, b\rangle \langle -, b| (\mathbb{1} \otimes A) + (\mathbb{1} \otimes A) |-, b\rangle \langle +, b|$ , aside from the identity matrix which only shifts the spectrum and induces a global phase in the dynamics.

Based on the four Hamiltonians  $H_1, H_2, H_3$ , and  $H_4$ , we can construct an Alternating Operator Ansatz, which is a direct translation of the approach in [24] into the QAOA framework [10]. Let us define the Ansatz as follows. Let  $p$  be the number of layers of alternating unitaries. For a set of variational parameters  $\theta_{k,j}$ ,  $k \in [p]$  and  $j \in [4]$ , we define the parameterized unitaries corresponding to the four Hamiltonians,  $U_j(\theta_{k,j}) := e^{-i\theta_{k,j} H_j}$ . Then our variational Ansatz is

$$U_4(\theta_{p,4})U_3(\theta_{p,3})U_2(\theta_{p,2})U_1(\theta_{p,1}) \dots U_4(\theta_{1,4})U_3(\theta_{1,3})U_2(\theta_{1,2})U_1(\theta_{1,1})|b\rangle.$$

This Ansatz contains explicit information of  $A$  and  $b$ , which avoids potential problems in variational algorithms discussed in Section III D. However, the suitability of this method for the use in near-term quantum computers depends on the difficulty of simulating the unitaries  $U_j(\theta_{k,j})$ . Given Assumptions 1 and 2, we can express the Hamiltonians as  $H_1 = \sum_{k,k'=1}^{K_A} \alpha_k \alpha_{k'} U_k U_{k'}$ ,  $H_2 = (\mathbb{1} \otimes U_b) |-, \bar{0}\rangle \langle -, \bar{0}| (\mathbb{1} \otimes U_b^\dagger)$ ,  $H_3 = \sum_{k,k'=1}^{K_A} \alpha_k \alpha_{k'} U_k (\mathbb{1} \otimes U_b) |+, \bar{0}\rangle \langle +, \bar{0}| (\mathbb{1} \otimes U_b^\dagger) U_{k'}$ , and  $H_4 = \sum_{k=1}^{K_A} \alpha_k (\mathbb{1} \otimes U_b) |+, \bar{0}\rangle \langle +, \bar{0}| (\mathbb{1} \otimes U_b^\dagger) (\mathbb{1} \otimes U_k) + (\mathbb{1} \otimes U_k) (\mathbb{1} \otimes U_b) |-, \bar{0}\rangle \langle +, \bar{0}| (\mathbb{1} \otimes U_b^\dagger)$ . As these operators are combinations of unitaries and projectors, Hamiltonian simulation for simple cases may be within the realm of near-term hardware. However, at this point, there are no guarantees on performance due to the potentially difficult optimization of the variational parameters  $\theta_{k,j}$ .

## D. Potential problems in variational algorithms for solving linear systems

Typical optimization for linear systems minimizing  $\|Ax - b\|_2^2$  is convex in  $x$ , and hence is easy to solve in principle. This is because the gradient is larger when we are further away from the optimal solution and the gradient always points in the descent direction. On the other hand, when we restrict to the non-convex constraint  $x = |x(\theta)\rangle$  with  $\theta \in \mathbb{R}^m$ , the optimization landscape is no longer convex and is poorly understood. We consider the following toy problem and show difficulties that arise in solving linear systems of equations. Let  $k \in \{0, 1\}^n$  be an arbitrary  $n$ -bit string. Let the problem be given by

$$A = (\sigma_x^{(1)})^{k_1} \otimes \dots \otimes (\sigma_x^{(n)})^{k_n}, \quad |b\rangle = |0\rangle^{\otimes n}.$$

The solution to the equation  $A|x\rangle = |b\rangle$  is simply  $|k\rangle$ . Note that  $A$  is sparse and the condition number of  $A$  is 1, hence existing quantum algorithm for linear systems [29–31] are able to solve this linear system efficiently.

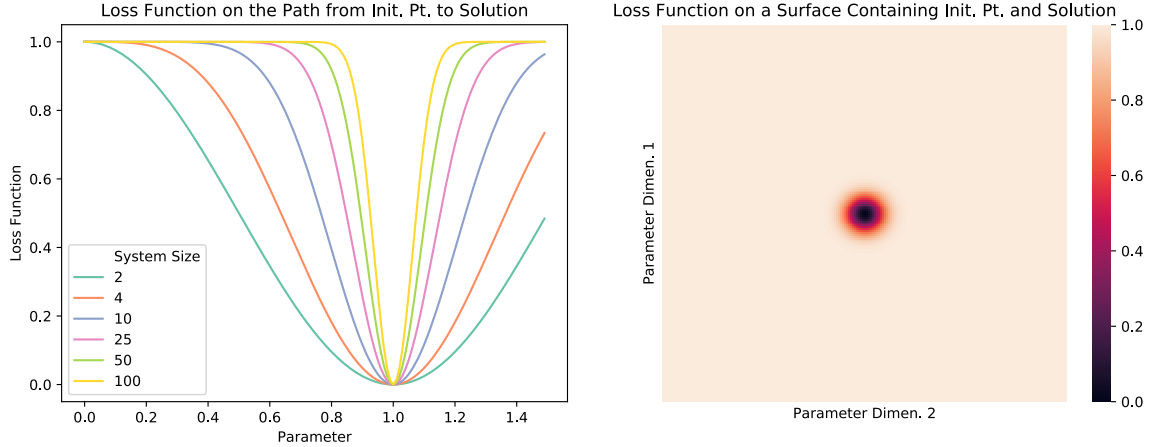


FIG. 1: The optimization landscape of variational linear system solver for  $k \in \{0,1\}^n$  with  $\|k\|_0 = \lceil n/2 \rceil$  and  $A = (\sigma_x^{(1)})^{k_1} \otimes \dots \otimes (\sigma_x^{(n)})^{k_n}$ ,  $|b\rangle = |\bar{0}\rangle$  using the variational Ansatz Eq. (2). Left: Here, we plot a one-dimensional cut through the high-dimensional landscape, tracing along a line connecting the initial point (parameter = 0) and the optimal solution (parameter = 1) for varying system size. We can clearly see the appearance of a plateau with the solution being a sharp valley at some point in the high-dimensional surface. Right: We plot the landscape on a surface that contains the initial point (bottom left corner with loss function = 1.0) and the optimal solution (the middle point with loss function = 0.0) for a system with  $n = 100$ . The loss function is near flat everywhere except a sharp hole in the middle that contains the solution.

Now assume a variational Ansatz  $|x(\theta)\rangle$  that contains the solution (up to global phase) for every  $k \in \{0,1\}^n$ . For example, one possible choice would be

$$|x(\theta)\rangle = e^{-i\theta_1\sigma_x^{(1)}} \otimes \dots \otimes e^{-i\theta_n\sigma_x^{(n)}} |\bar{0}\rangle, \quad (2)$$

with  $n$  variational parameters  $\theta$ . We now show that for both loss functions  $\|A|x\rangle - |b\rangle\|_2^2$  (the standard loss function) and  $\langle x|(A^2 - A|b\rangle\langle b|A)|x\rangle$  (the Hamiltonian loss function), no matter what the initial  $\theta$  is, the loss function will be flat at that point with an exponentially small slope under high probability. To show this, consider a polynomial-sized set of quantum states  $|\psi_1\rangle, \dots, |\psi_m\rangle$ , where  $m = O(\text{poly}(n))$ . Then, a randomly chosen  $k \in \{0,1\}^n$  will satisfy  $|\langle b|A|\psi_i\rangle| < 1/2^{n/4}$ ,  $\forall i \in \{1, \dots, m\}$  with probability at least  $1 - m/2^{n/2} \approx 1$ . This can be seen by the following argument. For each  $i$ , there are at most  $2^{n/2}$  entries in  $|\psi_i\rangle$  with absolute value  $\geq 1/2^{n/4}$ . So the probability of  $|\langle b|A|\psi_i\rangle| > 1/2^{n/4}$  is at most  $1/2^{n/2}$ . A union bound over all  $i = 1, \dots, m$  gives the desired result.

For  $\|A|x(\theta)\rangle - |b\rangle\|_2^2$ , consider an initial point  $\theta^0$ , the local expansion is

$$2 - 2\text{Re} \left\{ \langle b|A|x(\theta^0)\rangle \right\} - \sum_{i=1}^m 2\text{Re} \left\{ \langle b|A \frac{\partial}{\partial \theta_i} |x(\theta^0)\rangle \right\} \delta\theta_i.$$

Based on the previous property,  $\langle b|A \frac{\partial}{\partial \theta_i} |x(\theta^0)\rangle$  will be exponentially small for all  $i$  with high probability. Hence, around  $\theta^0$ , the loss function  $\|A|x(\theta)\rangle - |b\rangle\|_2^2$  is flat and has an almost constant value  $2 - 2\text{Re} \left\{ \langle b|A|x(\theta^0)\rangle \right\}$ . Now for  $\langle x(\theta)|(A^2 - A|b\rangle\langle b|A)|x(\theta)\rangle$ , pick an initial point  $\theta^0$ , the local expansion of the loss function at  $\theta^0$  is

$$1 - \langle x(\theta^0)|A|b\rangle\langle b|A|x(\theta^0)\rangle - \sum_{i=1}^m 2\text{Re} \left\{ \langle x(\theta^0)|A|b\rangle\langle b|A \frac{\partial}{\partial \theta_i} |x(\theta^0)\rangle \right\} \delta\theta_i.$$

We again have that  $\langle b|A \frac{\partial}{\partial \theta_i} |x(\theta^0)\rangle$  will be exponentially small for all  $i$  when the  $k$  defining  $A$  is sampled uniformly at random. We thus have the loss function is flat with a function value of  $1 - \langle x(\theta^0)|A|b\rangle\langle b|A|x(\theta^0)\rangle$  around  $\theta^0$ . The flat region is not a local minimum, but a plateau with large loss function.

This plateau problem holds no matter how the variational circuit for generating  $|x(\theta)\rangle$  is structured. For example, the circuit could be shallow, like in the example (2), and the behavior still appears. This behavior only becomes evident when the system size is larger, i.e.,  $n/4 \gg 1$ , but still within reach in the NISQ era [32]. A numerical experiment that demonstrates this behavior can be seen in Figure 1. From the figure, we can clearly see the appearance of the plateau as the system size grows larger.

Because the loss function landscape is essentially flat and there will be small errors due to statistical fluctuations in the quantum measurements, it would be very hard for existing optimization approaches to find the optimal solution efficiently even if there exists a solution in the Ansatz. For example, if we use variational

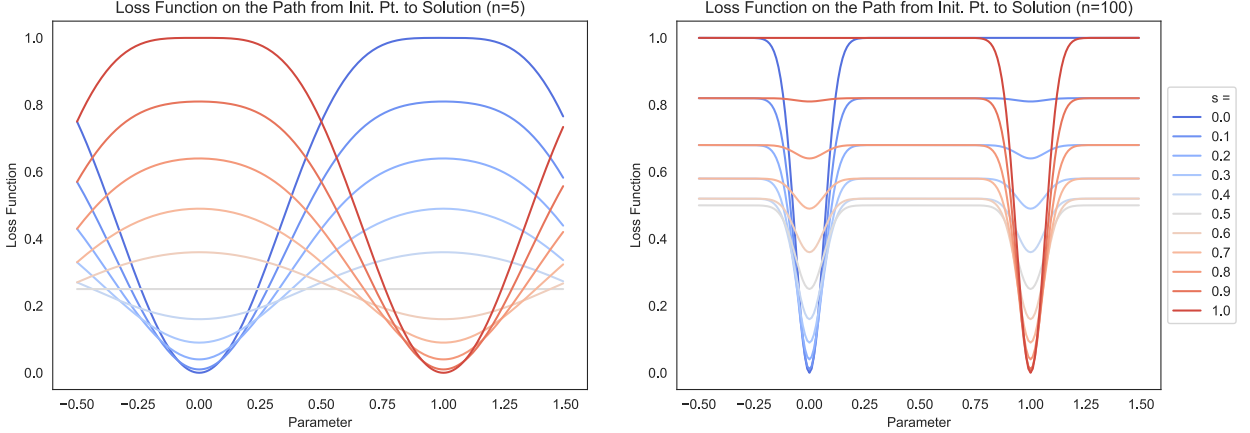


FIG. 2: The optimization landscape under adiabatic evolution ( $s$  from 0 to 1) to solve linear systems for  $k \in \{0, 1\}^n$  with  $\|k\|_0 = \lceil n/2 \rceil$  and  $A = (\sigma_x^{(1)})^{k_1} \otimes \dots \otimes (\sigma_x^{(n)})^{k_n}$ ,  $|b\rangle = |\bar{0}\rangle$  using the variational Ansatz Eq. (2). Here, we plot a one-dimensional slice through the high-dimensional landscape on a line passing through the initial point (parameter = 0) to the optimal solution (parameter = 1). Left: A system size of 5 qubits. Right: A system size of 100 qubits. For small system size, after  $s > 0.5$ , the variational parameter will be able to move toward the solution. For large system size, the adiabatic evolution will continue to be stuck at the initial point and end up at a plateau when  $s = 1.0$ .

imaginary time evolution to optimize the variational parameters, the same analysis shows that  $C(t)$  used in the propagation of  $\theta$  would be an exponentially small vector. This means even if  $C(t)$  is measured to exponential-precision (which already requires exponential time due to the statistical error in quantum measurements), the imaginary time propagation would still take exponential time to find the ground state.

One important note is that this plateau effect originates from a different cause compared to the barren plateau problem [23], which only appears in random quantum circuits with enough depth. The problem discussed here arises in *any fixed Ansatz* with a *polynomial number* of variational parameters. This means previous attempts to evade barren plateau may still fall into this problem. For example, one may perform adiabatic evolution to avoid barren plateau: we start with  $|x(\theta^0)\rangle = |-, b\rangle$ , which is the ground state of  $H(s=0) = A(0)(\mathbb{1} - |+, b\rangle\langle +, b|)A(0)$ , with  $A(s) = (1-s)Z \otimes \mathbb{I} + sX \otimes A$ ; then we gradually change  $s$  from 0 to 1 and use variational imaginary time evolution to maintain at the ground state. Intuitively, when we slightly change  $s$ , the ground state of  $H(s)$  will only shift a little, so performing imaginary time evolution allows us to closely follow the adiabatic path. This intuition is true in the original exponential-sized Hilbert space, but not true in the polynomial-sized variational parameter space. An intuition for why this is not true is because the topology in a polynomial-sized variational parameter space is very different from the original exponential-sized Hilbert space. For example, let  $a, b, c \in \{0, 1\}^n$ , and  $\epsilon \ll 1$ , then  $|a\rangle + \epsilon|b\rangle$  is close to  $|a\rangle + \epsilon|c\rangle$  in the original Hilbert space, but they may be very far away in the polynomial-sized variational parameter space.

Let us consider the same toy example,  $A = (\sigma_x^{(1)})^{k_1} \otimes \dots \otimes (\sigma_x^{(n)})^{k_n}$ ,  $|b\rangle = |0\rangle^{\otimes n}$ , and the loss function is

$$\langle x(\theta) | H(s) | x(\theta) \rangle = c(s) - (1-s)^2 f(\theta) - s^2 g(\theta) - 2s(1-s)h(\theta),$$

where  $c(s) = 1 - 2s + 2s^2$ ,  $f(\theta) = |\langle -, 0^n | x(\theta) \rangle|^2$ ,  $g(\theta) = |\langle +, b | (I \otimes A) | x(\theta) \rangle|^2$ ,  $h(\theta) = \frac{1}{2} \langle x(\theta) | -, 0^n \rangle \langle +, b | (I \otimes A) | x(\theta) \rangle + \frac{1}{2} \langle x(\theta) | (I \otimes A) | +, k \rangle \langle -, 0^n | x(\theta) \rangle$ . At  $s = 0$ , the optimum is  $|-, 0^n\rangle$ . At  $s = 1$ , the optimum is  $|+, k\rangle$ . The adiabatic evolution starts at  $s = 0$  with  $|x(\theta^0)\rangle = |-, 0^n\rangle$ . Suppose we change  $s$  from 0 to  $\Delta$ , then the loss function becomes  $c(\Delta) - (1 - \Delta)^2 f(\theta) - \Delta^2 g(\theta) - 2\Delta(1 - \Delta)h(\theta)$ . In the original Hilbert space, this loss function is quadratic in  $|x\rangle$  and we can simply move slightly in the direction of  $(I \otimes A)|+, b\rangle$ . However, in the polynomial-sized variational parameter space ( $m \ll 2^{n/2}$ ), the landscape of  $g(\theta)$  and  $h(\theta)$  will both be flat around  $\theta^0$  due to the inner product  $\langle +, b | (I \otimes A) | x(\theta) \rangle$  and the previous analysis. This means the loss function looks like  $c(\Delta) - (1 - \Delta)^2 f(\theta)$  around  $\theta^0$  and is minimized at  $|-, 0^n\rangle = |x(\theta^0)\rangle$ . So even if  $s$  has been changed to  $\Delta > 0$ , the variational parameter will still stay at  $\theta^0$ . The adiabatic evolution would hence always stay at  $|x(\theta^0)\rangle = |-, 0^n\rangle$  and fail to find the solution. An illustration of this analysis can be found in Figure 2.

The conclusion is that if we want to use variational algorithms with a pre-specified Ansatz to solve (sparse) linear systems of equations, the Ansatz must have a number of parameters that is of the order of  $2^{n/2}$ . Otherwise, we will encounter the problem discussed in this section. An alternative approach to circumvent this problem is to create an Ansatz that contains explicit application of  $A$ , such as  $e^{-iAt}$ , in its variational circuit. The Alternating Operator Ansatz proposed in Section III C is an example that may be able to go around this problem, but it fails to provide any guarantee and the optimization of variational parameters can be equally hard. In the next section, we aim to propose an approach that circumvents this problem and offers some provable guarantees.

## IV. ADAPTIVE ALTERNATING ALGORITHM FOR LINEAR SYSTEMS

### A. Classical combination of variational quantum states

To extend the reach of near-term quantum devices, we consider an approach that broaden the set of manipulable states in the  $N = 2^n$ -dimensional Hilbert space  $\mathcal{H}$ . Consider the set of variational quantum states  $\mathcal{V} = \{|\psi(\theta)\rangle \mid \theta \in \mathbb{R}^k\} \subset \mathcal{H}$  that can be created on near-term quantum devices, e.g., they have limited gate count, or have certain topology. Typical variational algorithms try to find the best  $|\psi(\theta)\rangle$  in  $\mathcal{V}$  by tuning  $\theta$ . However, there are two drawbacks with using typical variational algorithms.

- $\mathcal{V}$  may not be large enough to contain the solution. Such a drawback may often be the case in hardware-efficient Ansätze and even the Alternating Operator Ansatz discussed above.
- Even when  $\mathcal{V}$  contains the solution, the variational parameter  $\theta$  could be difficult to optimize. This problem can already be seen in the toy examples presented in previous sections.

Here, we improve on both drawbacks with a method called classical combination of variational quantum states (CQS). Most hybrid quantum-classical algorithms parameterize the quantum state with classical parameters, and have the quantum state created on the quantum processor. In classical combination of variational quantum states, we take a step further, and consider a hybrid quantum-classical state. We construct a state vector  $x \in \mathcal{H}$  as a quantum-classical hybrid,

$$x = \sum_{i=1}^m \alpha_i |\psi(\theta_i)\rangle, \text{ where } \alpha_1, \dots, \alpha_m \in \mathbb{C}, \theta_1, \dots, \theta_m \in \mathbb{R}^k,$$

where  $\alpha_i$  are the combination parameters and  $\theta_i$  are the usual variational parameters. Both parameters are stored on the classical processor. However, the state vector  $x \in \mathcal{H}$  is never created on the quantum processor. Furthermore  $x$  may not be normalized, so it is not a quantum state in general.

To manipulate  $x$  in variational quantum algorithms, the most important component is the ability to measure its expectation value for an observable  $O$ . We can simulate the expectation value  $x^\dagger O x$  by performing quantum measurements and classical post-processing, via the following steps.

1. Estimate  $\langle \psi(\theta_i) | O | \psi(\theta_j) \rangle$  using a modified Hadamard test (see Proposition 8 in Appendix A) on the quantum processor. The modified Hadamard test comes at the cost of preparing  $|\psi(\theta_i)\rangle$  and  $|\psi(\theta_j)\rangle$  in superposition using one additional ancilla.
2. Compute  $\sum_{i=1}^m \sum_{j=1}^m \alpha_i^* \alpha_j \langle \psi(\theta_i) | O | \psi(\theta_j) \rangle$  on the classical processor.

Suppose that  $x$  is a (normalized) quantum state. To create  $x$  on the quantum processor, we need at least  $\mathcal{O}(\log(m))$  ancilla qubits and  $m$  controlled unitaries that prepare all  $|\psi(\theta_i)\rangle, \forall i$  in superposition. Hence the improvement in terms of quantum resources using this hybrid quantum-classical state  $x$  is

$$\begin{aligned} \text{gate count: } & m \text{ times} \rightarrow 2 \text{ times,} \\ \text{ancilla count: } & \mathcal{O}(\log(m)) \rightarrow 1. \end{aligned}$$

The CQS method comes at the cost of many repetitions in quantum measurements. However, we do not need to maintain quantum coherence between measurements, hence it would be especially beneficial on noisy intermediate-scale quantum devices as the gate count is reduced  $m/2$ -fold. For example, when we consider a classical combination of 300 variational quantum states, then we can reduce the gate count by 150 times. On a near term quantum device, the gate count is often limited due to the error present in the device. Hence the space of possible variational quantum state  $\mathcal{V}$  that can be prepared without error on the quantum processor will be limited by the gate count. The classical combination of quantum states thus provides a considerable improvement upon the space of manipulable states on near-term quantum processors. An illustration of this idea is shown in Figure 3.

We now present the overview for the optimization of  $x \in \mathcal{H}$  to solve linear systems of equations. We adopt an adaptive alternating approach that avoids the optimization of  $\theta_i$  due to its complex optimization landscape. We start with  $m = 1$  and a  $|\psi(\theta_1)\rangle$ . Each iteration works as follows.

1. Solve for the optimal  $\alpha_1^*, \dots, \alpha_m^* \in \mathbb{C}$  with  $x(\alpha) = \sum_{i=1}^m \alpha_i |\psi(\theta_i)\rangle$ .
2. Find the next  $|\psi(\theta_{m+1})\rangle$  using  $x(\alpha^*) = \sum_{i=1}^m \alpha_i^* |\psi(\theta_i)\rangle$ .
3. Set  $m \leftarrow m + 1$ .

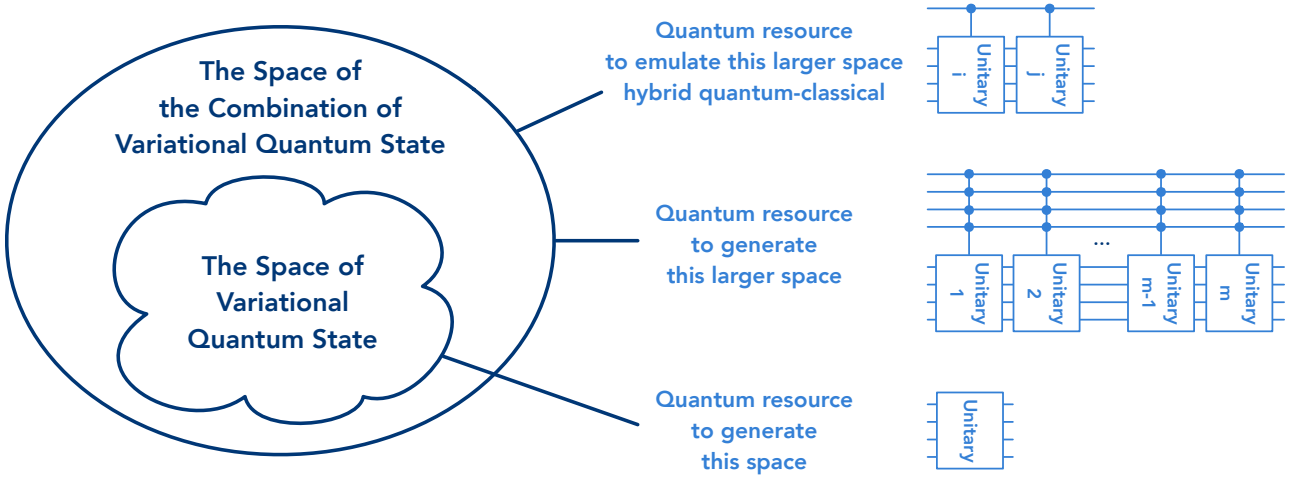


FIG. 3: Illustration of our *classical combination of variational quantum states* (CQS) approach. By considering subspaces spanned by  $m$  variational quantum states, we are able to represent a larger class of states in the Hilbert space  $\mathcal{H}$ . The basic concept is illustrated on the left-hand side. In order to generate states in the  $m$ -dimensional subspace, we have to increase the quantum resources  $m$ -fold ( $m$  times more gates and  $O(\log(m))$  ancilla qubits that jointly control the unitaries). This case is illustrated by the middle picture on the right-hand side. Using a hybrid quantum-classical emulation, we can operate in this larger space using only a single additional ancilla qubit and twice as many gates, as illustrated in the top picture on the right-hand side.

## B. Optimization of combination parameters

We first focus on the case where we have selected a good set of  $|\psi(\theta_1)\rangle, \dots, |\psi(\theta_m)\rangle$ , e.g.,  $A^{-1}|b\rangle \in \text{span}\{|\psi(\theta_1)\rangle, \dots, |\psi(\theta_m)\rangle\}$ , and we want to optimize over  $\alpha_1, \dots, \alpha_m$ . We will show that the optimization of  $\alpha_1, \dots, \alpha_m$  will always find the optimal solution. This is in stark contrast to the optimization over  $\theta_i$ , which can result in plateaus and local minima. To avoid complication of notations, we will let  $|u_i\rangle = |\psi(\theta_i)\rangle$  further on. In order to solve linear systems of equations, the standard loss function is

$$\|Ax - |b\rangle\|_2^2 = x^\dagger A^\dagger Ax - 2\text{Re}\{\langle b|Ax\} + 1.$$

Given  $x = \sum_{i=1}^m \alpha_i |u_i\rangle$ , we can reduce the optimization in an exponentially large space  $x \in \mathcal{H}$  to an optimization over  $m$  variables. Let  $V = (v_1, \dots, v_m)$  with the column vectors  $v_i = A|u_i\rangle$ . We can now simply express the left-hand side of the linear system as  $Ax = \sum_{i=1}^m \alpha_i A|u_i\rangle = V\alpha$ . Thus, we would like to minimize

$$\|V\alpha - |b\rangle\|_2^2 = \alpha^\dagger V^\dagger V\alpha - 2\text{Re}\{\langle q| \alpha\} + 1,$$

where we introduced  $q_i = \langle i|V^\dagger|b\rangle = \langle u_i|A^\dagger|b\rangle$ . We obtain a simple regression problem for the combination parameters  $\alpha$  with the kernel matrix  $(V^\dagger V)_{ij} = \langle u_i|A^\dagger A|u_j\rangle$ . We can cast this quadratic optimization problem with complex variable  $\alpha \in \mathbb{C}^m$  to a real optimization problem  $\min_z z^T Q z - 2r^T z + 1$ , by letting  $z = [\text{Re}\{\alpha\}, \text{Im}\{\alpha\}] \in \mathbb{R}^{2m}$  and let

$$Q = \begin{pmatrix} \text{Re}\{V^\dagger V\} & \text{Im}\{V^\dagger V\} \\ \text{Im}\{V^\dagger V\} & \text{Re}\{V^\dagger V\} \end{pmatrix}, \quad r = [\text{Re}\{q\}, \text{Im}\{q\}].$$

Once all the input quantities  $Q$  and  $r$  are determined, such a regression problem can be solved with standard methods for convex quadratic programming, such as the interior point method. The inputs  $Q$  and  $r$  can be measured on a quantum computer using the strategies in Appendix A and B. However, such measurements result in an erroneous estimate of the quantities. The error will translate into an error in the loss function and the proposed solution for the combination parameters  $\alpha$ . Using standard results in random matrix theory, we are able to achieve a rigorous bound on the error of the obtained solution, see Proposition 1. See also Appendix B for a detailed analysis and Proposition 9 for the complete statement.

**Proposition 1** (informal version). *We can find an  $\hat{\alpha} \in \mathbb{C}^m$  such that it is  $\epsilon$ -close to optimal,*

$$\left\| A \left( \sum_i \hat{\alpha}_i u_i \right) - |b\rangle \right\|_2^2 \leq \min_{\alpha_1, \dots, \alpha_m \in \mathbb{R}} \left\| A \left( \sum_i \alpha_i u_i \right) - |b\rangle \right\|_2^2 + \epsilon,$$

using  $\mathcal{O}(m^3/\epsilon)$  measurements on the quantum device.

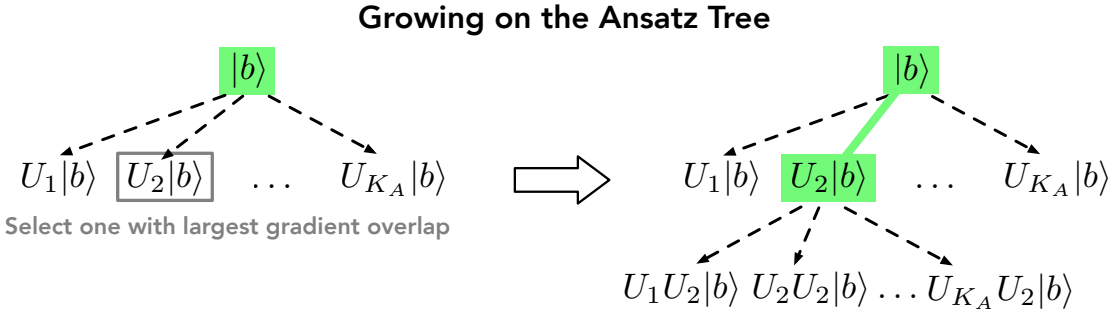


FIG. 4: Illustration of the Ansatz tree and the adaptive growing strategy. The green region is the current subspace. On the left-hand side, we select a node that is a child of the nodes in the green region and that has the largest overlap with the gradient, here  $U_2|b\rangle$ . The right-hand side shows the tree after adding adding the new element to the subspace.

A natural question that arises is whether the problem of solving linear system will become much easier when we consider optimization over a small subspace  $\text{span}(|u_1\rangle, |u_2\rangle, \dots, |u_m\rangle)$ . Here we show that finding a near-optimal combination parameters in a subspace is BQP-complete. See Proposition 10 in Appendix B for the complete statement and proof.

**Proposition 2** (informal version). *Finding the combination parameters of  $|u_1\rangle, |u_2\rangle, \dots, |u_m\rangle$  to minimize  $\|A \sum_{i=1}^m \alpha_i |u_i\rangle - b\|_2^2$  is BQP-complete.*

### C. Adaptive approach for finding the subspace

While we have shown good theoretical properties in the case where the subspace is fixed, such as a guarantee for finding a near-optimal solution in the subspace and BQP-completeness, the requirement of knowing a subspace that approximately contains the solution  $x$  can be restrictive. Here, we propose an adaptive approach that grows the subspace by exploring the space of solutions on an Ansatz tree. A near-optimal solution is guaranteed to be found after we include enough nodes on the Ansatz tree, however this number may be very large in the worst case.

The Ansatz tree is constructed as follows. The node at the root of the tree corresponds to the quantum state  $|b\rangle$ . For every node we can construct its children corresponding to quantum states generated by the matrix  $A$ . Let a particular node correspond to some quantum state  $|\psi\rangle$ . Then the children of this node are given by  $U_1|\psi\rangle, \dots, U_{K_A}|\psi\rangle$ . An illustration is shown in Figure 4. At the start, the subspace  $S$  contains only the root, i.e.,  $S = \{|b\rangle\}$ . In each step, we will solve for the optimal  $x = \sum_{|\psi_i\rangle \in S} \alpha_i |\psi_i\rangle$  using the optimization of combination parameters discussed in Section IV B. Then we will find a node neighboring to nodes in the subspace  $S$ , such that the node has the largest overlap with the gradient  $Ax - |b\rangle$ . The gradient overlap can be computed efficiently using the Hadamard test via Proposition 6. We call this procedure for growing the tree the *gradient expansion heuristics*.

In general, we are guaranteed to find a near-optimal solution after enough iterations, see Proposition 3. However, without the use of the gradient expansion heuristics, the number of nodes we have to include may be very large. The gradient expansion heuristics can be useful in reducing the number of nodes we have to include in the subspace.

**Proposition 3.** *For a fixed  $\epsilon > 0$ , and  $A = \sum_{k=1}^{K_A} \beta_k U_k$  with  $\rho(A) \leq 1, \rho(A^{-1}) \leq \kappa$ . By selecting all nodes  $\{u_1, \dots, u_m\}$  on the Ansatz tree with depth at most  $O(\kappa \log(\kappa/\epsilon))$ , we have*

$$\min_{\alpha_1, \dots, \alpha_m \in \mathbb{R}} \left\| A \left( \sum_i \alpha_i u_i \right) - b \right\|_2^2 \leq \min_{x \in \mathbb{C}^{2^n}} \|Ax - b\|_2^2 + \epsilon.$$

Instead of the loss function from Definition 1, one may want to use the regularized version  $\frac{1}{2} \|x\|_2^2 + \|Ax - b\|_2^2$ . This version is common in statistics and machine learning, and is known as Tikhonov regularization [33], or ridge regression [34]. For this regularized linear system of equations, a polynomial number of iterations is enough to guarantee the performance of the solution even in the worst case, see Proposition 4.

**Proposition 4.** *For a fixed  $\epsilon > 0$ , and  $A = \sum_{k=1}^{K_A} \beta_k U_k$  with  $\rho(A) \leq 1$ . By selecting all nodes  $\{u_1, \dots, u_m\}$  on the Ansatz tree with depth at most  $\lceil \log(1/2\epsilon) / \log(1/(2 - \sqrt{3})) \rceil$ , we have*

$$\min_{\alpha_1, \dots, \alpha_m \in \mathbb{R}} \left( \frac{1}{2} \left\| \sum_i \alpha_i u_i \right\|_2^2 + \left\| A \left( \sum_i \alpha_i u_i \right) - b \right\|_2^2 \right) \leq \min_{x \in \mathbb{C}^{2^n}} \left( \frac{1}{2} \|x\|_2^2 + \|Ax - b\|_2^2 \right) + \epsilon.$$

For example, when  $\epsilon = 0.01$ , we have  $m \leq K_A^5$  and the depth is at most 5.

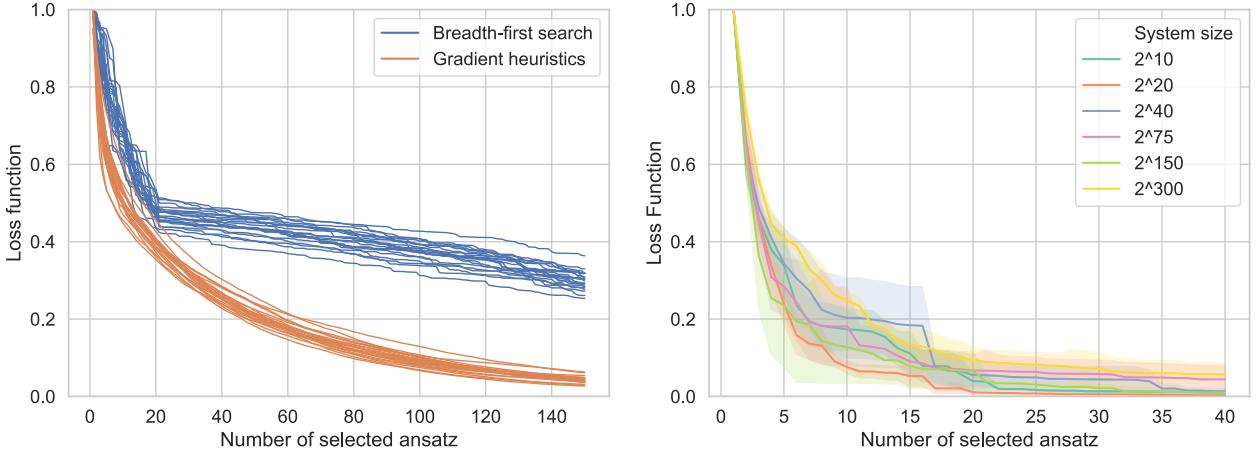


FIG. 5: Numerical experiments on the adaptive alternating algorithm for solving linear systems of equations. Left: Comparison of breadth-first search and the gradient expansion heuristics for adding nodes on the Ansatz tree to the subspace. We consider solving linear systems with a system size of  $256 \times 256$  where  $A$  is generated by sampling random weighted sum of Haar-random unitaries. Matrices  $A$  generated this way have a large condition number (as large as the system size), so a large number of Ansatz states are needed to find the solution. Each line represents an independent run. Right: Solving linear systems over a wide range of system sizes (from  $2^{10} \times 2^{10}$  to  $2^{300} \times 2^{300}$ ). For efficient classical simulation, the linear systems are generated as random weighted sums of Pauli strings, i.e., tensor product of Pauli operators. The shaded areas represent the standard deviation over five independent runs.

The proofs for both propositions are given in Appendix C. As an alternative to the adaptive tree search approach, one could also select a subspace by performing Hamiltonian simulation. More precisely, one could choose a set of Ansatz states as follows

$$\left\{ e^{-iAt} |b\rangle \mid t = \frac{\epsilon j}{\kappa \log(\kappa/\epsilon)}, j = -J, \dots, J \right\},$$

where  $J = \Theta\left(\frac{\kappa^2 \log(\kappa/\epsilon)}{\epsilon}\right)$  and  $\kappa$  is an upper-bound on the condition number of  $A$ . This set of Ansätze is of size  $\Theta(\kappa^2 \log(\kappa/\epsilon)/\epsilon)$  and the number of gates to generate each Ansatz is of size  $O(\kappa \log(\kappa/\epsilon))$  (assuming each application of  $A$  takes constant number of gates). This is less near-term compared to the adaptive approach based on Ansatz tree due to the need of Hamiltonian simulation. However, by optimizing the combination parameters over this set of quantum state Ansätze, we are guaranteed to find the solution for  $Ax = |b\rangle$  because this set of Ansätze can be used to perform Fourier approximation to  $A^{-1}|b\rangle$  [31]. It improves upon existing quantum algorithms for solving linear systems of equations [24] by reducing the circuit depth and gate count from  $O(\kappa \log(\kappa/\epsilon)/\epsilon)$  to  $O(\kappa \log(\kappa/\epsilon))$  and using only one additional ancilla for performing Hadamard test. As an example, when  $\epsilon = 0.01$ , we would achieve an 100-times reduction in the quantum circuit depth.

#### D. Numerical experiments for the adaptive alternating algorithm

We now present numerical experiments for the adaptive algorithm. The experiments are shown in Figure 5. In Figure 5 (left), we compare the use of gradient expansion heuristics with the use of a breadth-first search that simply includes every node on the Ansatz tree layer-by-layer. We consider randomly generated linear systems of size  $256 \times 256$ . We generate a random linear system by selecting several unitary matrices  $U_1, \dots, U_S$  from the Haar measure, random scalars  $\alpha_1, \dots, \alpha_S$  from uniform distribution  $[-2, 2]$  and let  $A = \sum_{i=1}^S \alpha_i (U_i + U_i^\dagger)$ . This construction guarantees that  $A$  is Hermitian and is a weighted sum of unitary matrices. The condition number generated this way is very large (in the order of the system size). In particular, we consider  $S = 10$  (hence  $A$  is a sum of 20 unitaries). A clear improvement can be seen when using the gradient expansion heuristics. This gradient heuristics converges quickly to the optimal point. On the other hand, including every node on the Ansatz tree results in a very slow convergence after the first 20 rounds (this includes the first layer of the Ansatz tree).

In Figure 5 (right), we consider a special class of (sparse) linear systems that are extremely large. In particular, we consider system sizes ranging from  $2^{10} \times 2^{10}$  to  $2^{300} \times 2^{300}$  to investigate whether our new approach suffers from the plateau issue discussed in Section III D. To facilitate classical simulation, we consider  $A \in \mathbb{C}^{2^n \times 2^n}$  with efficient Pauli decomposition, i.e.,  $A = \sum_{i=1}^S \alpha_i P_1^{(i)} \otimes \dots \otimes P_n^{(i)}$ , where  $P_j^{(i)}$  is a single-qubit Pauli operator (including the identity). In addition, we set  $|b\rangle = |0^n\rangle$ . To generate a random matrix  $A$ , we sample each  $\alpha_i$

from the uniform distribution over  $[-2, 2]$ , and a random tensor product of Pauli operators from the uniform distribution over  $4^n$  possible choices. Here, we consider  $S = 8$ . Note that when  $S = 1$  and we only sample from  $I$  or  $X$  in the Pauli string, then it recovers the toy problem that leads to a new plateau issue discussed in Section III D. From Figure 5, we can see that this approach circumvents the plateau issue and has a clear convergence over an extremely wide range of system sizes.

## V. DISCUSSION

The work provides algorithms for solving linear systems on near-term quantum computers. The flavor of the presented algorithms is two-fold. The first set of algorithms are variational in nature and draw their inspiration from other variational quantum algorithms for quantum chemistry [7, 26, 35, 36] and quantum optimization [10, 37, 38]. For such algorithms, the quantum computer implements a single wavefunction Ansatz which is dependent on a set of variational parameters, usually in a non-linear fashion. The type of Ansatz in this setting can, in the extreme cases, be linear system-independent (agnostic) or fully linear system-dependent. As the agnostic case is useful for example when limitations of the hardware are dominating the overall implementation, such Ansätze have also been called “hardware efficient” [9]. On the other hand, the dependent Ansatz takes into account the linear system at the cost of requiring Hamiltonian simulation which increases the overall complexity of implementing such an Ansatz in a near-term quantum processor.

The second set of approaches are based on classical combination of variational quantum states (CQS). The method is inspired from the basic concept of diversification and robustness. Using a single class of methods can provide only limited benefits when compared to combining multiple different methods and using the best parts of each. This method introduces a new set of combination parameters to add together different variational quantum states. The combination is emulated classically rather than represented directly on the quantum computer. Hence, the method increases the overall expressiveness and power of the Ansatz without the need of additional quantum resources. We can use the variational states such as the ones presented in the first part, and also others yet to be developed. Our CQS approach is reminiscent of the linear combination of atomic orbitals (LCAO) approach in quantum chemistry. A molecule consists of a collection of atoms. For each atom, we have a set of electronic states (orbitals), which describe how the electrons occupy the space around the nucleus. Such atomic orbitals are then linearly-combined to obtain molecular electronic states. The combination coefficients are found by an optimization procedure similar to the one discussed in this work, taking into account overlaps between atomic orbitals and matrix elements of the Hamiltonian with respect to the atomic orbitals.

To avoid the complexity of optimizing the variational parameters, which often involves an ill-shaped optimization landscape with plateaus and local minima, we proposed an adaptive alternating approach that alternates between solving for the optimal solution in a subspace and growing the subspace adaptively on an Ansatz tree. This adaptive alternating approach is inspired by the Krylov subspace method in solving linear systems. Krylov subspace is a subspace spanned by  $\{b, Ab, A^2b, \dots, A^{r-1}b\}$ , which is similar to the Ansatz tree we defined. The Krylov subspace method solves for the optimal solution in the subspace and increases  $r$  if the obtained solution is not good enough. A popular variant of Krylov subspace method for linear systems is the conjugate gradient method [39]. The Ansatz tree is also reminiscent of the coupled-cluster Ansatz in quantum chemistry [40–43], which systematically takes into account higher and higher orders of the electron correlation at the cost of increasing the complexity of preparing the Ansatz.

We have performed numerical experiments solving exponentially large linear systems with sizes up to  $2^{300} \times 2^{300}$ . These experiments are achieved by considering a special class of linear systems that allows efficient simulation of the proposed quantum algorithm on a classical computer. To achieve actual quantum advantage, we require either  $A$  to be a sum of unitaries that cannot be simulated efficiently on a classical computer or  $b$  to be a quantum state generated by some quantum circuit. It should be noted that there will always be a trade-off between how near-term the quantum algorithm is (the required quantum coherence, entanglement, and interference) and how much quantum advantage we can expect from executing the quantum algorithm. An important future direction would be a detailed analysis on the performance of the proposed algorithms under the effect of decoherence and imperfections of real-world quantum devices. We believe the synthesis and future improvement of the proposed ideas can provide real benefits for solving linear systems when quantum computers achieve sizes of 50-70 high quality qubits.

*Note added:* After completion of this paper, a few related works on reducing the quantum resources for linear systems were posted very recently [44–46]. These works have some overlap with our discussion on using variational algorithms to solve linear systems. Some of the proposed variational algorithms are similar to our Agnostic Ansatz and fall into the newly observed plateau issues in Section III D. Others are similar to our Alternating Operator Ansatz and require Hamiltonian simulation of  $A$  and  $b$ .

## VI. ACKNOWLEDGEMENTS

We would like to thank Yudong Cao, John Preskill, Ansis Rosmanis, Miklos Santha, Thomas Vidick, and Zhikuan Zhao for valuable discussions. H.H. is supported by the Kortschak Scholars Program and thanks the hospitality of the Centre for Quantum Technologies. K.B. acknowledges the CQT Graduate Scholarship. P.R. acknowledges support from Singapore's Ministry of Education and National Research Foundation and Baidu.

---

[1] J. Preskill, arXiv preprint arXiv:1203.5813 (2012).

[2] S. Aaronson and L. Chen, arXiv preprint arXiv:1612.05903 (2016).

[3] A. W. Harrow and A. Montanaro, *Nature* **549**, 203 (2017).

[4] C. Neill, P. Roushan, K. Kechedzhi, S. Boixo, S. V. Isakov, V. Smelyanskiy, A. Megrant, B. Chiaro, A. Dunsworth, K. Arya, et al., *Science* **360**, 195 (2018).

[5] S. Aaronson and A. Arkhipov, in *Proceedings of the forty-third annual ACM symposium on Theory of computing* (ACM, 2011), pp. 333–342.

[6] M. J. Bremner, R. Jozsa, and D. J. Shepherd, *Proceedings of the Royal Society A: Mathematical, Physical and Engineering Sciences* **467**, 459 (2010).

[7] A. Peruzzo, J. McClean, P. Shadbolt, M.-H. Yung, X.-Q. Zhou, P. J. Love, A. Aspuru-Guzik, and J. L. Obrien, *Nature communications* **5**, 4213 (2014).

[8] J. R. McClean, J. Romero, R. Babbush, and A. Aspuru-Guzik, *New Journal of Physics* **18**, 023023 (2016).

[9] A. Kandala, A. Mezzacapo, K. Temme, M. Takita, M. Brink, J. M. Chow, and J. M. Gambetta, *Nature* **549**, 242 (2017).

[10] E. Farhi, J. Goldstone, and S. Gutmann, arXiv preprint arXiv:1411.4028 (2014).

[11] E. Farhi and A. W. Harrow, arXiv preprint arXiv:1602.07674 (2016).

[12] R. Tibshirani, *Journal of the Royal Statistical Society: Series B (Methodological)* **58**, 267 (1996).

[13] E. Candes, J. Romberg, and T. Tao, arXiv preprint math/0409186 (2004).

[14] J. C. Lagarias, J. A. Reeds, M. H. Wright, and P. E. Wright, *SIAM Journal on Optimization* **9**, 112 (1998).

[15] Y. Li and S. C. Benjamin, *Physical Review X* **7**, 021050 (2017).

[16] S. McArdle, T. Jones, S. Endo, Y. Li, S. C. Benjamin, and X. Yuan, *npj Quantum Information* **5**, 1 (2019).

[17] E. Farhi, J. Goldstone, S. Gutmann, and M. Sipser, arXiv preprint quant-ph/0001106 (2000).

[18] S. Lloyd, *Science* **273**, 1073 (1996).

[19] D. W. Berry, A. M. Childs, R. Cleve, R. Kothari, and R. D. Somma, *Physical Review Letters* **114**, 090502 (2015).

[20] D. W. Berry, A. M. Childs, and R. Kothari, in *2015 IEEE 56th Annual Symposium on Foundations of Computer Science* (IEEE, 2015), pp. 792–809.

[21] G. H. Low and I. L. Chuang, *Physical Review Letters* **118**, 010501 (2017).

[22] G. H. Low and I. L. Chuang, *Quantum* **3**, 163 (2019).

[23] J. R. McClean, S. Boixo, V. N. Smelyanskiy, R. Babbush, and H. Neven, *Nature communications* **9**, 4812 (2018).

[24] Y. Subaşı, R. D. Somma, and D. Orsucci, *Physical Review Letters* **122**, 060504 (2019).

[25] S. McArdle, T. Jones, S. Endo, Y. Li, S. Benjamin, and X. Yuan, arXiv:1804.03023 (2018).

[26] D. Wecker, M. B. Hastings, and M. Troyer, *Physical Review A* **92**, 042303 (2015).

[27] A. Garcia-Saez and J. Latorre, arXiv preprint arXiv:1806.02287 (2018).

[28] R. S. Smith, M. J. Curtis, and W. J. Zeng, *A practical quantum instruction set architecture* (2016).

[29] A. W. Harrow, A. Hassidim, and S. Lloyd, *Phys. Rev. Lett.* **103**, 150502 (2009).

[30] A. Ambainis, arXiv preprint arXiv:1010.4458 (2010).

[31] A. M. Childs, R. Kothari, and R. D. Somma, *SIAM Journal on Computing* **46**, 1920 (2017).

[32] J. Preskill, *Quantum* **2**, 79 (2018).

[33] A. Y. Ng, in *Proceedings of the twenty-first international conference on Machine learning* (ACM, 2004), p. 78.

[34] A. E. Hoerl and R. W. Kennard, *Technometrics* **12**, 55 (1970).

[35] P. J. O'Malley, R. Babbush, I. D. Kivlichan, J. Romero, J. R. McClean, R. Barends, J. Kelly, P. Roushan, A. Tranter, N. Ding, et al., *Physical Review X* **6**, 031007 (2016).

[36] J. I. Colless, V. V. Ramasesh, D. Dahlen, M. S. Blok, M. Kimchi-Schwartz, J. McClean, J. Carter, W. De Jong, and I. Siddiqi, *Physical Review X* **8**, 011021 (2018).

[37] N. Moll, P. Barkoutsos, L. S. Bishop, J. M. Chow, A. Cross, D. J. Egger, S. Filipp, A. Fuhrer, J. M. Gambetta, M. Ganzhorn, et al., *Quantum Science and Technology* **3**, 030503 (2018).

[38] Z. Wang, S. Hadfield, Z. Jiang, and E. G. Rieffel, *Physical Review A* **97**, 022304 (2018).

[39] J. R. Shewchuk et al., *An introduction to the conjugate gradient method without the agonizing pain* (1994).

[40] J. Čížek, *The Journal of Chemical Physics* **45**, 4256 (1966).

[41] H. J. Monkhorst, *International Journal of Quantum Chemistry* **12**, 421 (1977).

[42] G. D. Purvis III and R. J. Bartlett, *The Journal of Chemical Physics* **76**, 1910 (1982).

[43] R. J. Bartlett, *The Journal of Physical Chemistry* **93**, 1697 (1989).

[44] X. Xu, J. Sun, S. Endo, Y. Li, S. C. Benjamin, and X. Yuan, arXiv preprint arXiv:1909.03898 (2019).

[45] C. Bravo-Prieto, R. LaRose, M. Cerezo, Y. Subasi, L. Cincio, and P. J. Coles, arXiv preprint arXiv:1909.05820 (2019).

[46] D. An and L. Lin, arXiv preprint arXiv:1909.05500 (2019).

[47] A. S. Bandeira, R. Van Handel, et al., *The Annals of Probability* **44**, 2479 (2016).

## Appendix A: Measurements

**Lemma 1.** Let  $\epsilon > 0$  and  $P_k$  be a certain Pauli string over  $n$  qubits. Let multiple copies of an arbitrary  $n$ -qubit quantum state  $|\psi\rangle$  be given. The expectation value  $\langle\psi|P_k|\psi\rangle$  can be determined to additive accuracy  $\epsilon$  with failure probability at most  $\delta$  using  $\mathcal{O}\left(\frac{1}{\epsilon^2} \log\left(\frac{1}{\delta}\right)\right)$  copies of  $|\psi\rangle$ .

*Proof.* A single measurement obtains the outcome  $m_{\pm} = \pm 1$ . We have  $\langle\psi|P_k|\psi\rangle = pm_{+} + (1-p)m_{-} = 2p - 1$ , where  $p$  is the probability of measuring  $+1$ . To estimate this probability, perform independent trials of the Bernoulli test. Each trial has expectation value  $p$ . We use the statistic  $M_+/M$ , where  $M_+$  is the number of positive outcomes over  $M$  trials. For the error estimate, we require  $P[|2M_+/M - 1 - \langle\psi|P_k|\psi\rangle| \geq \epsilon] \leq \delta$  from which the number of measurements is  $\mathcal{O}\left(\frac{1}{\epsilon^2} \log\left(\frac{1}{\delta}\right)\right)$  via Hoeffding's inequality.  $\square$

**Proposition 5** (Swap test). *Given multiple copies of  $n$ -qubit quantum states  $|u\rangle$  and  $|v\rangle$ . There is a quantum algorithm that determines the overlap  $|\langle v|u\rangle|^2$  to additive accuracy  $\epsilon$  with failure probability at most  $\delta$  using  $\mathcal{O}\left(\frac{1}{\epsilon^2} \log\left(\frac{1}{\delta}\right)\right)$  copies and  $\tilde{\mathcal{O}}\left(\frac{1}{\epsilon^2} \log\left(\frac{1}{\delta}\right)\right)$  operations.*

*Proof.* Use an ancilla and perform a controlled swap  $\frac{1}{\sqrt{2}}(|0\rangle + |1\rangle)|u\rangle|v\rangle \rightarrow \frac{1}{\sqrt{2}}(|0\rangle|u\rangle|v\rangle + |1\rangle|v\rangle|u\rangle)$ . Performing a Hadamard on the ancilla obtains  $\frac{1}{2}(|0\rangle(|u\rangle|v\rangle + |v\rangle|u\rangle) + |1\rangle(|u\rangle|v\rangle - |v\rangle|u\rangle)) = |\xi\rangle$ . Now measure the ancilla in  $Z$ . The expectation value is  $\langle\xi|Z|\xi\rangle = \frac{1}{4}(\langle u|v\rangle + \langle v|u\rangle)(|u\rangle|v\rangle + |v\rangle|u\rangle) - \frac{1}{4}(\langle u|v\rangle - \langle v|u\rangle)(|u\rangle|v\rangle - |v\rangle|u\rangle) = |\langle v|u\rangle|^2$ .  $\square$

We can also measure the real and imaginary part separately under a different input model.

**Proposition 6** (Hadamard test). *Assume the controlled state preparation  $U_{\text{prep}} = |0\rangle\langle 0| \otimes U_{v_0} + |1\rangle\langle 1| \otimes U_{v_1}$ , with  $U_{v_j}|\bar{0}\rangle = |v_j\rangle$ . There is a quantum algorithm that determines  $\text{Re}\{\langle v_0|v_1\rangle\}$  and  $\text{Im}\{\langle v_0|v_1\rangle\}$  to additive accuracy  $\epsilon$  with failure probability at most  $\delta$  using  $\mathcal{O}\left(\frac{1}{\epsilon^2} \log\left(\frac{1}{\delta}\right)\right)$  applications of  $U_{\text{prep}}$  and  $\tilde{\mathcal{O}}\left(\frac{1}{\epsilon^2} \log\left(\frac{1}{\delta}\right)\right)$  operations.*

*Proof.* Use an ancilla prepared in  $(|0\rangle + \alpha|1\rangle)/\sqrt{2}$  with  $\alpha = 1$  or  $\alpha = i$ . Apply  $U_{\text{prep}}$  to obtain  $\frac{1}{\sqrt{2}}(|0\rangle|v_0\rangle + \alpha|1\rangle|v_1\rangle)$ . Another Hadamard on the ancilla obtains  $\frac{1}{2}(|0\rangle(|v_0\rangle + \alpha|v_1\rangle) + |1\rangle(|v_0\rangle - \alpha|v_1\rangle)) = |\xi\rangle$ . Now measure the ancilla in  $Z$ . The expectation value is  $\langle\xi|Z|\xi\rangle = \frac{1}{2}(\alpha\langle v_0|v_1\rangle + \alpha^*\langle v_1|v_0\rangle)$ . If  $\alpha = 1$ , then  $\langle\xi|Z|\xi\rangle = \text{Re}\{\langle v_0|v_1\rangle\}$ . If  $\alpha = i$ , then  $\langle\xi|Z|\xi\rangle = \text{Im}\{\langle v_0|v_1\rangle\}$ .  $\square$

**Proposition 7** (Measuring the Hamiltonian Loss Function). *Given Assumptions 2 on the unitary decomposition of  $A$ . The loss function  $\langle x|A^2|x\rangle - \langle x|A|b\rangle\langle b|A|x\rangle$  can be estimated efficiently on a quantum computer.*

*Proof.* For the first term, we expand  $A^2 = \sum_k \sum_l \alpha_k \alpha_l U_k U_l$ . Then we measure each terms  $\langle x|U_k U_l|x\rangle$  individually using the Hadamard test in Proposition 6 with  $|v_0\rangle = |x\rangle$  and  $|v_1\rangle = U_k U_l|x\rangle$ . For the second term, we expand  $A = \sum_k \alpha_k U_k$  and estimate  $\langle b|A|x\rangle = \sum_k \alpha_k \langle b|U_k|x\rangle$ . We use the Hadamard test in Proposition 6 with  $|v_0\rangle = |b\rangle$  and  $|v_1\rangle = U_k|x\rangle$  to estimate each term. Then  $\langle x|A|b\rangle\langle b|A|x\rangle = |\langle b|A|x\rangle|^2$  can be estimated.  $\square$

**Proposition 8** (Modified Hadamard test). *Assume the controlled state preparation  $U_{\text{prep}} = |0\rangle\langle 0| \otimes U_{v_0} + |1\rangle\langle 1| \otimes U_{v_1}$ , with  $U_{v_j}|\bar{0}\rangle = |v_j\rangle$  is an  $n$ -qubit state. Given an observable  $O = U^\dagger D U \in \mathbb{C}^{2^n \times 2^n}$ , where  $U$  is a unitary matrix that can be implemented efficiently as a quantum circuit,  $D$  is a real diagonal matrix, and  $D_{ii}$  can be computed efficiently as a classical function  $f : 2^n \rightarrow \mathbb{R}$ . Both  $\text{Re}\{\langle v_0|O|v_1\rangle\}$  and  $\text{Im}\{\langle v_0|O|v_1\rangle\}$  can be estimated efficiently on a quantum computer.*

*Proof.* Use an ancilla prepared in  $(|0\rangle + \alpha|1\rangle)/\sqrt{2}$  with  $\alpha = 1$  or  $\alpha = i$ . Apply  $UU_{\text{prep}}$  to obtain  $\frac{1}{\sqrt{2}}(|0\rangle \otimes U|v_0\rangle + \alpha|1\rangle \otimes U|v_1\rangle)$ . Another Hadamard on the ancilla gives us  $|\xi\rangle = \frac{1}{2}(I \otimes U)(|0\rangle(|v_0\rangle + \alpha|v_1\rangle) + |1\rangle(|v_0\rangle - \alpha|v_1\rangle))$ . Now measure the ancilla in  $Z$  to get  $z_a \in \{\pm 1\}$  and the rest of the state in the computational basis to get  $b \in \{0, 1\}^n$ . We then compute  $z_a f(b)$ . The expectation value is  $\langle\xi|Z \otimes D|\xi\rangle = \frac{1}{2}(\alpha\langle v_0|O|v_1\rangle + \alpha^*\langle v_1|O|v_0\rangle)$ . If  $\alpha = 1$ , then  $\langle\xi|Z \otimes D|\xi\rangle = \text{Re}\{\langle v_0|O|v_1\rangle\}$ . If  $\alpha = i$ , then  $\langle\xi|Z \otimes D|\xi\rangle = \text{Im}\langle v_0|O|v_1\rangle$ .  $\square$

## Appendix B: Detailed analysis on optimizing combination coefficients

The necessary quantum measurements for obtaining the inputs  $Q, r$  needed to solve the combination coefficients is discussed in the following lemma.

**Lemma 2.** *Given the unitary decomposition of matrix  $A$  from Assumption 2, the circuit for  $|b\rangle$  via Assumption 1, and the circuit for creating  $|u_i\rangle$  be  $W_i$ . Assume that controllable unitaries of all involved unitaries can be constructed. Then, we can obtain a single estimate of  $(V^\dagger V)_{ij} = \langle u_i|A^\dagger A|u_j\rangle$  and  $q_i = \langle u_i|A^\dagger|b\rangle$  from  $O(K_A^2), O(K_A)$  quantum measurements, where the magnitude of each estimate is bounded by  $O((\sum_{i=1}^{K_A} |\alpha_k|)^2), O(\sum_{i=1}^{K_A} |\alpha_k|)$  respectively.*

*Proof.* Note that  $\langle u_i | A^\dagger A | u_j \rangle = \sum_{k,k'=1}^{K_A} \alpha_k \alpha_{k'} \langle \bar{0} | W_i^\dagger U_k^\dagger U_{k'} W_j | \bar{0} \rangle$ , where  $|\bar{0}\rangle = |0\rangle^{\otimes n}$ . Construct the unitaries  $U_{\text{prep},k,k'} = |0\rangle\langle 0| \otimes \mathbb{1} + |1\rangle\langle 1| \otimes W_i^\dagger U_k^\dagger U_{k'} W_j$ . Use the Hadamard test via Proposition 6 to obtain a single estimate for  $\langle \bar{0} | W_i^\dagger U_k^\dagger U_{k'} W_j | \bar{0} \rangle$ . The absolute value of the estimate is bounded by  $O(1)$  because the estimate for the real and imaginary part are both bounded by 1. We can estimate  $\langle \bar{0} | W_i^\dagger U_k^\dagger U_{k'} W_j | \bar{0} \rangle$  for all  $k, k'$  using  $O(K_A^2)$  quantum measurements. Then we obtained an estimate for  $\text{Re} \{ \langle u_i | A^\dagger A | u_j \rangle \}$ , where the absolute value is bounded by  $O((\sum_{i=1}^{K_A} |\alpha_k|)^2)$ . Similar steps and constructing the unitaries  $U_{\text{prep},k,b} = |0\rangle\langle 0| \otimes \mathbb{1} + |1\rangle\langle 1| \otimes W_i^\dagger U_k^\dagger U_b$  allow us to obtain an estimate for  $\langle u_i | A^\dagger | b \rangle$  with absolute value bounded by  $O(\sum_{i=1}^{K_A} |\alpha_k|)$  using  $O(K_A)$  quantum measurements.  $\square$

The following proposition summarizes the required number of measurements to achieve a good solution. This proposition focuses on real optimization where the variable  $z$  is real.

**Proposition 9.** *Consider a quadratic function  $L(z) = z^T Q z - 2r^T z + s$ , where  $Q$  is positive definite and  $z \in \mathbb{R}^m$ . Let  $z^* = \arg \min_{z \in \mathbb{R}^m} L(z)$ . By measuring each entry of  $Q$  and  $r$  independently where each measurement results in a value bounded by  $B$ , then we can find  $z$  such that*

$$L(z) - L(z^*) \leq \epsilon,$$

with  $\mathcal{O} \left( B^2 m^3 \|Q\| \|Q^{-1}\|^2 (1 + \|z^*\|)^2 / \epsilon \right)$  measurements.

*Proof.* Due to statistical fluctuations in the measurements, we can only obtain an estimate of  $Q$  and  $r$ , which we denote as  $\hat{Q}$  and  $\hat{r}$ . Note that  $s$  does not matter because it just shifts the function value without changing the optimal point. We estimate each entry in  $Q, r$  independently. Because each measurement on an entry results in a value bounded by  $B$ , the average of  $\mathcal{O}(B^2 T)$  measurements on a single entry gives us a sub-gaussian random variable with variance  $\mathcal{O}(1/T)$ . By performing  $\mathcal{O}(B^2 m^2 T)$  measurements, we obtain an independent estimate for all the entries in  $Q, r$ . Standard results in random matrix theory [47] give  $\|\hat{Q} - Q\| \leq \mathcal{O}(\sqrt{m/T})$  and  $\|\hat{r} - r\| \leq \mathcal{O}(\sqrt{m/T})$  with high probability.

Now, we solve for  $z$  by minimizing  $\hat{L}(z) = z^T \hat{Q} z - 2\hat{r}^T z$ . This results in  $z = \hat{Q}^{-1} \hat{r}$ . Similarly,  $z^* = Q^{-1} r$ . Thus we have  $\hat{Q} z - Q z + Q z - Q z^* = \hat{r} - r$ . This gives  $(z - z^*) = Q^{-1}(\hat{r} - r - (\hat{Q} - Q)z)$ . Hence  $\|z - z^*\| \leq \|Q^{-1}\| (\|\hat{r} - r\| + \|\hat{Q} - Q\| \|z\|) \leq \|Q^{-1}\| \|\hat{r} - r\| + \|Q^{-1}\| \|\hat{Q} - Q\| \|z^*\| + \|Q^{-1}\| \|\hat{Q} - Q\| \|z - z^*\|$ . This gives

$$\|z - z^*\| \leq \frac{\|Q^{-1}\| (\|\hat{r} - r\| + \|\hat{Q} - Q\| \|z^*\|)}{1 - \|Q^{-1}\| \|\hat{Q} - Q\|} \leq \sqrt{\epsilon / \|Q\|}.$$

The last inequality requires setting  $T$  to be  $\mathcal{O} \left( m \|Q\| \|Q^{-1}\|^2 (1 + \|z^*\|)^2 / \epsilon \right)$ , such that  $1 - \|Q^{-1}\| \|\hat{Q} - Q\| \geq 1/2$  and  $\|Q^{-1}\| (\|\hat{r} - r\| + \|\hat{Q} - Q\| \|z^*\|) \leq \frac{1}{2} \sqrt{\epsilon / \|Q\|}$ . Because  $L(z)$  has zero gradient at  $z^*$ , we have

$$L(z) - L(z^*) \leq \|Q\| \|z - z^*\|^2 \leq \epsilon.$$

The total number of measurements is

$$\mathcal{O}(B^2 m^2 T) = \mathcal{O} \left( B^2 m^3 \|Q\| \|Q^{-1}\|^2 (1 + \|z^*\|)^2 / \epsilon \right).$$

$\square$

The following is a detailed statement on the BQP-completeness for optimizing combination coefficients.

**Proposition 10.** *Given a Hermitian matrix  $A$  that have an efficient unitary decomposition and each entry can be efficiently computed classically, a quantum circuit that generates  $|b\rangle$ , and two quantum circuits for  $|u_1\rangle, |u_2\rangle$ . It is BQP-complete to output  $\hat{\alpha}_1, \hat{\alpha}_2 \in \mathbb{C}$ , such that*

$$\left\| A \sum_{i=1}^2 \hat{\alpha}_i |u_i\rangle - |b\rangle \right\|_2^2 \leq \min_{\alpha_1, \alpha_2 \in \mathbb{C}} \left\| A \sum_{i=1}^2 \alpha_i |u_i\rangle - |b\rangle \right\|_2^2 + \epsilon. \quad (\text{B1})$$

*Proof.* Consider a quantum circuit consisting of two-qubit gates  $U_1, \dots, U_T$  acting on  $n$  qubits. Determining the probability of measuring 0 in the first qubit after applying  $U_1, \dots, U_T$  on  $|0^n\rangle$ ,  $P_0 \equiv \langle 0^n | U_1^\dagger \dots U_T^\dagger (|0\rangle\langle 0| \otimes I \otimes \dots \otimes I) U_T \dots U_1 | 0^n \rangle$ , up to small error is BQP-complete. The same is true for the probability of measuring 1,  $P_1 \equiv \langle 0^n | U_1^\dagger \dots U_T^\dagger (|1\rangle\langle 1| \otimes I \otimes \dots \otimes I) U_T \dots U_1 | 0^n \rangle$ . We now construct a linear systems of dimension  $2^{n+1}$ , which acts on a  $n+1$  qubit system. The matrix  $A$  is a simple controlled-NOT gate, controlled by the second

qubit and acting on the first qubit. Note that  $A$  is both Hermitian and unitary, and each entry can be efficiently computed classically. The three quantum states are given by

$$|b\rangle = |0\rangle \otimes U_T \dots U_1 |0^n\rangle, \quad |u_1\rangle = |0\rangle \otimes U_T \dots U_1 |0^n\rangle, \quad |u_2\rangle = |1\rangle \otimes U_T \dots U_1 |0^n\rangle.$$

We can easily see that  $\langle b|A|u_1\rangle = P_0$ . Similarly,  $\langle b|A|u_2\rangle = P_1$ . Suppose there is an algorithm that can efficiently find  $\hat{\alpha}_1, \hat{\alpha}_2 \in \mathbb{C}$  that satisfies Equation (B1). We now show that  $\hat{\alpha}_1, \hat{\alpha}_2$  can be used to infer  $P_0, P_1$ . By expansion, we have

$$\left\| A \left( \sum_{i=1}^2 \alpha_i |u_i\rangle \right) - |b\rangle \right\|_2^2 = |\alpha_1|^2 + |\alpha_2|^2 - 2\text{Re} \{ \alpha_1 \langle b|A|u_1\rangle + \alpha_2 \langle b|A|u_2\rangle \} + 1.$$

Using  $\langle b|A|u_1\rangle = P_0, \langle b|A|u_2\rangle = P_1$ , we have  $\left\| A \sum_{i=1}^2 \alpha_i |u_i\rangle - |b\rangle \right\|_2^2 = |\alpha_1 - P_0|^2 + |\alpha_2 - P_1|^2 + (1 - P_0^2 - P_1^2)$ . The optimal combination parameters are  $\alpha_1 = P_0, \alpha_2 = P_1$ . Hence Equation (B1) can be rewritten as

$$|\hat{\alpha}_1 - P_0|^2 + |\hat{\alpha}_2 - P_1|^2 + (1 - P_0^2 - P_1^2) \leq (1 - P_0^2 - P_1^2) + \epsilon \implies |\hat{\alpha}_1 - P_0|^2 + |\hat{\alpha}_2 - P_1|^2 \leq \epsilon.$$

This means the algorithm can use  $\hat{\alpha}_1, \hat{\alpha}_2$  to determine  $P_0$  and  $P_1$ , which is BQP-complete.  $\square$

### Appendix C: Provable guarantee for the Ansatz tree approach

We provide proof for the following propositions. This is a simple extension and variation of known results on using polynomial approximation of  $1/x$  to solve linear systems of equations [31].

**Proposition 11** (Same as Proposition 3). *For a fixed  $\epsilon > 0$ ,  $A = \sum_{k=1}^{K_A} \beta_k U_k$  with  $\rho(A) \leq 1, \rho(A^{-1}) \leq \kappa$ , and  $b$  with  $b^\dagger b = 1$ . By selecting all nodes  $\{u_1, \dots, u_m\}$  on the Ansatz tree with depth at most  $O(\kappa \log(\kappa/\epsilon))$ , we have*

$$\min_{\alpha_1, \dots, \alpha_m \in \mathbb{R}} \left\| A \left( \sum_i \alpha_i u_i \right) - b \right\|_2^2 \leq \min_{x \in \mathbb{C}^{2^n}} \|Ax - b\|_2^2 + \epsilon.$$

*Proof.* By including all nodes  $\{u_1, \dots, u_m\}$  on the Ansatz tree with depth at most  $O(\kappa \log(\kappa/\epsilon))$ , the subspace contains  $p(A)b$  for any polynomial  $p(\cdot)$  with degree at most  $O(\kappa \log(\kappa/\epsilon))$ . In Lemma 14 in [31], it was shown that there exists a set of constants  $p_j, \forall j = 0, \dots, j_0$  such that  $p(z) = \sum_{j=0}^{j_0} p_j z^j$  is  $\epsilon$ -close to  $z^{-1}$  in the domain  $D_\kappa = [-1, -1/\kappa] \cup [1/\kappa, 1]$ , where  $j_0 = 2\sqrt{\kappa^2 \log(2\kappa/\epsilon) \log(8\kappa^2 \log(2\kappa/\epsilon)/\epsilon)} + 1 = O(\kappa \log(\kappa/\epsilon))$ . Using the condition that  $\rho(A) \leq 1$  and  $\rho(A^{-1}) \leq \kappa$ , we know that all the eigenvalues of  $A$  lie in the domain  $D_\kappa$ . Because  $p(z)$  is  $\epsilon$ -close to  $z^{-1}$  in the domain  $D_\kappa$ , we thus have  $\|p(A) - A^{-1}\| \leq \epsilon$ . This implies that  $\|p(A)b - A^{-1}b\| \leq \|p(A) - A^{-1}\| \leq \epsilon$ . Hence there exists a set of combination parameters  $\hat{\alpha}_1, \dots, \hat{\alpha}_m \in \mathbb{R}$  set according to the coefficients  $p_j$  in the polynomial  $p(x)$ , such that  $\hat{x} = \sum_i \hat{\alpha}_i u_i$  satisfies  $\|\hat{x} - A^{-1}b\| \leq \epsilon$ . So

$$\min_{\alpha_1, \dots, \alpha_m \in \mathbb{R}} \left\| A \left( \sum_i \alpha_i u_i \right) - b \right\|_2^2 \leq \|A\hat{x} - b\|_2^2 \leq \rho(A)^2 \|\hat{x} - A^{-1}b\|_2^2 \leq \epsilon^2 = \min_{x \in \mathbb{C}^{2^n}} \|Ax - b\|_2^2 + \epsilon^2.$$

The last equality uses the fact that  $x = A^{-1}b$  satisfy  $\|Ax - b\|_2 = 0$ . Note that we actually achieve  $\epsilon^2$  error, which is better than  $\epsilon$  since  $\epsilon < 1$ .  $\square$

**Proposition 12** (Same as Proposition 4). *For a fixed  $\epsilon > 0$ , and  $A = \sum_{k=1}^{K_A} \beta_k U_k$  with  $\rho(A) \leq 1$ . By selecting all nodes  $\{u_1, \dots, u_m\}$  on the Ansatz tree with depth at most  $\lceil \log(1/2\epsilon) / \log(1/(2 - \sqrt{3})) \rceil$ , we have*

$$\min_{\alpha_1, \dots, \alpha_m \in \mathbb{R}} \left( \frac{1}{2} \left\| \sum_i \alpha_i u_i \right\|_2^2 + \left\| A \left( \sum_i \alpha_i u_i \right) - b \right\|_2^2 \right) \leq \min_{x \in \mathbb{C}^{2^n}} \left( \frac{1}{2} \|x\|_2^2 + \|Ax - b\|_2^2 \right) + \epsilon.$$

*Proof.* We first diagonalize  $A$  to be  $VDV^\dagger$ , where  $D$  is diagonal and  $V$  is a unitary matrix. We also set  $N = 2^n$  to be the system size. The eigenvalues of  $A$  are denoted as  $\lambda_i, \forall i = 1, \dots, N$ . We set  $\tilde{b} = V^\dagger b$  and note that  $\sum_{i=1}^N |\tilde{b}_i|^2 = 1$ , as  $b$  is normalized by assumption. We consider a rotated  $x, \tilde{x} = V^\dagger x \in \mathbb{C}^N$ . Using  $\tilde{x}$ , the loss function  $\frac{1}{2} \|x\|_2^2 + \|Ax - b\|_2^2$  can be written as

$$\sum_{i=1}^N \left( \frac{1}{2} |\tilde{x}_i|^2 + |\lambda_i \tilde{x}_i - \tilde{b}_i|^2 \right).$$

We can minimize this expression analytically as

$$\tilde{x}_i = \frac{2\lambda_i \tilde{b}_i}{2\lambda_i^2 + 1} \in \mathbb{C}, \forall i = 1, \dots, N.$$

Plugging this optimal solution into the loss function yields

$$\sum_{i=1}^N |\tilde{b}_i|^2 \left( \frac{1}{2} y_i^2 + (\lambda_i y_i - 1)^2 \right),$$

where  $y_i = 2\lambda_i/(2\lambda_i^2 + 1) \in \mathbb{R}$ . We now consider the space of all linear combinations of  $A^k b, \forall k = 0, \dots, K_0$ , which is a subspace of  $\text{span}(u_1, \dots, u_m)$ . This space is written as  $\left\{ \sum_{k=0}^{K_0} p_k A^k b \right\}$ . In this subspace, the loss function can be written as

$$\frac{1}{2} \left\| \sum_k p_k D^k \tilde{b} \right\|_2^2 + \left\| \sum_k p_k D^{k+1} \tilde{b} - \tilde{b} \right\|_2^2 = \sum_{i=1}^N |\tilde{b}_i|^2 \left( \frac{1}{2} \left( \sum_k p_k \lambda_i^k \right)^2 + \left( \lambda_i \sum_k p_k \lambda_i^k - 1 \right)^2 \right).$$

We now analyze how accurate a polynomial  $\sum_k p_k x^k$  can approximate  $2x/(2x^2 + 1)$  within  $[-1, 1]$ . Due to the condition that  $\rho(A) \leq 1$ , we only care about the range  $[-1, 1]$ . The approximation can be done by performing Chebyshev decomposition of the function  $x/(x^2 + 1/2)$ ,

$$\frac{x}{x^2 + 1/2} = \sum_{k=0,1,2,\dots} c_k T_{2k+1}(x),$$

where  $T_{2k+1}(x)$  is  $(2k+1)$ -th Chebyshev polynomial of the first kind (which is of degree  $2k+1$ ). And we have the following recursive formula for  $c_k, \forall k = 0, 1, 2, \dots$ ,

$$c_k = (-2 + \sqrt{3})^k \left( 1 - \frac{1}{\sqrt{3}} \right).$$

If we truncate the Chebyshev expansion at  $\lfloor (K_0 - 1)/2 \rfloor$  (the degree is at most  $K_0$ ), then

$$\sup_{x \in [-1, 1]} \left| \frac{x}{x^2 + 1/2} - \sum_{k=0}^{\lfloor (K_0 - 1)/2 \rfloor} c_k T_{2k+1}(x) \right| \leq \sum_{k=\lfloor (K_0 - 1)/2 \rfloor + 1}^{\infty} |c_k| \leq \frac{(2 - \sqrt{3})^{K_0/2} \left( 1 - \frac{1}{\sqrt{3}} \right)}{\sqrt{3} - 1} \equiv \eta.$$

By choosing  $p_k$  according to  $c_k$  and the Chebyshev polynomial coefficients, we have

$$\left| y_i - \sum_{k=0}^{K_0} p_k \lambda_i^k \right| \leq \eta, \forall i = 1, \dots, N.$$

Then using  $\frac{1}{2} z^2 + (\lambda_i z - 1)^2 = \frac{1}{2} y_i^2 + (\lambda_i y_i - 1)^2 + (\frac{1}{2} + \lambda_i^2)(z - y_i)^2, \forall z \in \mathbb{R}$ , we have

$$\frac{1}{2} \left( \sum_k p_k \lambda_i^k \right)^2 + \left( \lambda_i \sum_k p_k \lambda_i^k - 1 \right)^2 \leq \frac{1}{2} y_i^2 + (\lambda_i y_i - 1)^2 + \left( \frac{1}{2} + \lambda_i^2 \right) \eta^2, \forall i = 1, \dots, N.$$

Using the fact that  $|\lambda_i| \leq 1$  and  $\sum_i |\tilde{b}_i|^2 = 1$ , we have

$$\sum_{i=1}^N |\tilde{b}_i|^2 \left( \frac{1}{2} \left( \sum_k p_k \lambda_i^k \right)^2 + \left( \lambda_i \sum_k p_k \lambda_i^k - 1 \right)^2 \right) \leq \min_{x \in \mathbb{C}^{2n}} \left( \frac{1}{2} \|x\|_2^2 + \|Ax - b\|_2^2 \right) + \frac{3}{2} \eta^2.$$

Now we want  $\frac{3}{2} \eta^2 \leq \epsilon$  by choosing a large enough  $K_0$ . Using  $\eta = \frac{(2 - \sqrt{3})^{K_0/2}}{\sqrt{3}}$ , we need  $(2 - \sqrt{3})^{K_0} \leq 2\epsilon$ . By choosing  $K_0 \geq \log(1/2\epsilon)/\log(1/(2 - \sqrt{3}))$ , we are guaranteed to have

$$\min_{\alpha_1, \dots, \alpha_m \in \mathbb{R}} \left( \frac{1}{2} \left\| \sum_i \alpha_i u_i \right\|_2^2 + \left\| A \left( \sum_i \alpha_i u_i \right) - b \right\|_2^2 \right) \leq \min_{x \in \mathbb{C}^{2n}} \left( \frac{1}{2} \|x\|_2^2 + \|Ax - b\|_2^2 \right) + \epsilon.$$

□

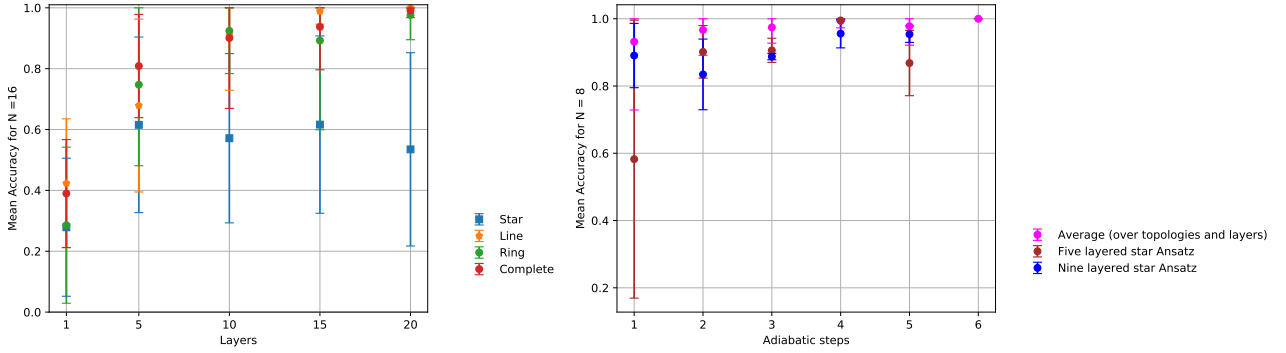


FIG. 6: Numerical experiments on solving linear systems using Agnostic Ansätze. Left: The mean accuracy versus circuit layer depth for various Ansätze employed to solve linear systems for  $N = 16$  is shown. The mean accuracy goes to unity for line graph, ring graph and complete graph Ansätze with a 20-layer circuit. The star-graph Ansatz performs worst and eventually levels at accuracy 0.6. Right: We implement the adiabatic-assisted VQE (AAVQE) approach for  $N = 8$  and see improvement over standard VQE (adiabatic steps = 1) over an average of all Ansätze and number of layers. Employing more adiabatic steps also improves the mean accuracy. For example, the mean accuracy for the five and nine layered star Ansätze improves to 1.0 as we increase the number of adiabatic steps from 1 to 6. The dots represent the mean accuracy and the bars represent the spread corresponding to a standard deviation with the upper and lower cutoffs as 1 and 0 respectively.

#### Appendix D: Experiments on solving linear systems using Agnostic Ansätze

We discuss our experiments on solving linear systems using the Agnostic Ansatz in detail. We focus on solving the real-valued version of Eq. (1). By construction, our Agnostic Ansatz is constrained to explore the solution vector in the real subspace of the appropriate Hilbert space. The two real gates we use are the single-qubit rotation around the  $y$ -axis for every qubit with tunable angle (the variational parameter) and the controlled NOT (CNOT) gate. Thus, a single layer of our  $n$ -qubit variational circuit consists of  $n$  variational parameters and a certain pattern of CNOT gates. We implement various types of Agnostic Ansätze depending on how the CNOT gates are applied. The topology of a quantum computer favours a particular arrangement of CNOT gates over another and our exploration for different Ansätze is motivated by the same. Here, we enumerate the different variational Ansätze. We label our qubits from 1 to  $n$  and denote the same by  $[1, \dots, n]$ . The CNOT gate between qubit  $i$  (control) and  $j$  (target) will be denoted by  $C(i, j)$ .

1. Star Ansatz: The qubit numbered 1 is always the control, while target ranges over all  $i \in [2, \dots, n]$ . In other words, we apply  $C(1, i)$  for all  $i \in [2, \dots, n]$ .
2. Line Ansatz: The Ansatz contains  $C(i, i+1)$  for every  $i \in [1, \dots, n-1]$ .
3. Ring Ansatz: It is similar to the line Ansatz with the difference that there is an extra CNOT gate at the boundary, i.e.,  $C(n, 1)$ .
4. Complete graph Ansatz: We implement  $C(i, j)$  for every  $i, j \in [1, \dots, n]$  such that  $i \neq j$ .

We have conducted numerical experiments on Rigetti quantum virtual machine where the linear systems are generated randomly over different system sizes ( $N = 2, 4, 8, 16$ ). Some of the numerical results can be seen in Figure 6. The figure of merit is mean accuracy, which is the average fidelity of the output vector and the solution over 100 independent runs. In Figure 6 (Left), we present the use of standard VQE for solving linear systems with  $N = 16$ . We can see a rise in overall performance as we increase the number of layers. The mean accuracy goes to unity for most CNOT gate patterns except for the star graph. The performance for the star graph starts improving but soon levels at mean accuracy of 0.6.

In Figure 6 (Right), we show the adiabatic-assisted VQE approach for  $N = 8$ . The purple/magenta data points are an average over all the topologies and different layers. We can see an improvement by roughly 10% using AAVQE (adiabatic steps = 6) over standard VQE (adiabatic steps = 1). We can also see that as we increase the number of adiabatic steps, the performance of AAVQE becomes better. The mean accuracy for all settings considered here becomes very close to unity as we increase the number of adiabatic steps to 6. Furthermore, the standard deviation around the mean accuracy goes below  $10^{-2}$ . As such, most of the settings were able to achieve the accuracy of close to 1.0 in AAVQE, which is not achieved with standard VQE (adiabatic steps = 1).